Texas A&M University

Department of

OCEANOGRAPHY

THE EQUATORIAL UNDERCURRENT, THE SOUTH EQUATORIAL COUNTERCURRENT, AND THEIR EXTENSIONS IN THE SOUTH PACIFIC OCEAN EAST OF THE GALAPAGOS ISLANDS DURING FEBRUARY-MARCH, 1967

Warren B. White

Office of Naval Research
Contract Nonr 2119(04)

Reference 69-4-T
May 1969

Project 286-3

Research Conducted
through the
Texas A&M University
Research Foundation
College Station, Texas

The Texas A&M University
DEPARTMENT OF OCEANOGRAPHY
College Station, Texas

Research Conducted Through The
TEXAS A & M RESEARCH FOUNDATION

THE EQUATORIAL UNDERCURRENT, THE SOUTH EQUATORIAL COUNTERCURRENT, AND THEIR EXTENSIONS IN THE SOUTH PACIFIC OCEAN EAST OF THE GALAPAGOS ISLANDS DURING FEBRUARY-MARCH, 1967

by

Warren B. White

This research was sponsored by the Office of Naval Research under Contract Nonr 2119(04) with the Texas A & M Research Foundation.

Office of Naval Research Contract Nonr 2119(04)
A&M Project 286-3
REFERENCE 69-4T
May 1969

PREFACE

This essay was written by Warren B. White in partial fulfillment of the requirements for the degree of Master of Science in Oceanography at Texas A&M University. The essay presents results of a study completed under the direction of John D. Cochrane and supported by the Texas A & M Research Foundation and the Office of Naval Research. The data for this study were obtained during a cruise sponsored by the Office of Naval Research and the National Science Foundation.

ABSTRACT

During February and March 1967, oceanographic observations taken by the R/V ALAMINOS east of the Galapagos Islands and north of 15°S covered the region more completely than previous cruises. The Equatorial Undercurrent was present as two branches, one north and the other south of the equator. This study deals with the circulation and water in the region south of the equator. They are studied by means of vertical sections, station curves, and distributions of properties on isanosteric surfaces from 120 to 280 cl/t. At selected locations volume transports are calculated.

The south branch of the Equatorial Undercurrent extended east between 2° and 4°S from the Galapagos Islands to the coast of Peru. There near 5°S, the flow turned west and reached to about 84°W, where it divided. While some of the flow continued west out of the region near 5°S, the greater part turned south, extended to about 10°S, and returned to the coast. There the flow turned south to form the Peru-Chile Undercurrent, which extended out of the region at 15°S. The Equatorial Undercurrent and its extensions were characterized by a marked thermostad between 150 and 190 cl/t.

Between 6° and 13°S, the South Equatorial Countercurrent entered the region. At 120 cl/t, the flow lay primarily between 11°

and 13°S, but from 160 cl/t upward the main eastward flow was between 6° and 8°S. In that zone, the eastward transport was largest. The current extended east to 86°W, where some of the flow joined the westward flow near 5°S. The remainder continued east to 84°W, where it joined the southward flow leading into the Peru-Chile Undercurrent.

A westward extension of the Chile Current passed through the region to the south of the South Equatorial Countercurrent. Between these two currents, the lowest oxygen values of the region were encountered between 150 and 180 cl/t. Nearer the coast, an offshoot of the Chile Current extended north to 11°S, where, below 180 cl/t, it turned east to contribute to the Peru-Chile Undercurrent.

ACKNOWLEDGEMENTS

The author wishes to express his appreciation to Professor John D. Cochrane for his guidance and assistance in preparing this essay. This study was supported largely by the Office of Naval Research under Contract Nonr 2119(04) with the Texas A & M Research Foundation.

TABLE OF CONTENTS

LIST OF TABLES

LIST OF FIGURES

CHAPTER I

INTRODUCTION

What happens to the Equatorial Undercurrent east of the Galapagos Islands has been a subject of interest since the discovery of the Undercurrent by Cromwell, Montgomery, and Stroup (1954). Observations in this region up to 1962 were summarized by Montgomery (1962), who reported that the "Undercurrent is usually absent or weak within this sector". According to Wyrtki (1966), the Undercurrent disintegrates west of the Islands and its water spreads north and south, with some of the water reaching to the northern coast of Peru. Cochrane and Zuta (1969), using data taken by the R/V ALAMINOS in February-March 1967, found the Equatorial Undercurrent east of the Islands divided into two branches, one north and the other south of the equator, both of which extended nearly to the coast of South America. The present study, based upon the same data used by Cochrane and Zuta, is concerned with the description of the south branch of the Equatorial Undercurrent, the closely associated portion of the South Equatorial Countercurrent, and their extensions in the region east of

The citations on the following pages follow the style of the Journal of Marine Research.

the Galapagos Islands.

This study is based on hydrographic data taken by the R/V ALAMINOS during the EASTROPAC studies of the eastern intertropical Pacific Ocean. The cruise lasted from January 21 to April 10, 1967, traversing a region (shown in figure 1) from 10°N to 15°S, from the coast of South America west to 89°W near the Galapagos Islands. The present study utilizes only data south of 2°N.

The eastern equatorial Pacific Ocean was visited previously by a number of major expeditions, none of which obtained a detailed coverage of the region under study. The SHELLBACK Expedition (1952) made its measurements primarily south of 5°S, with one meridional transect extending north along 85°W (Wooster and Cromwell, 1958). The EASTROPIC Expedition (1955) made most of its measurements north of 5°S adjacent to the coast of Ecuador (Bennett, 1963). The STEP-I Expedition (1960) concentrated its efforts in the region south of 5°S, with one meridional transect extending along 95°W (Wooster and Gilmartin, 1961).

The method for this study is determined, in part, by the location and shape of the study region, which is bounded on the east by the South American continent and on the north by the equator. Since little motion was indicated across the equator,

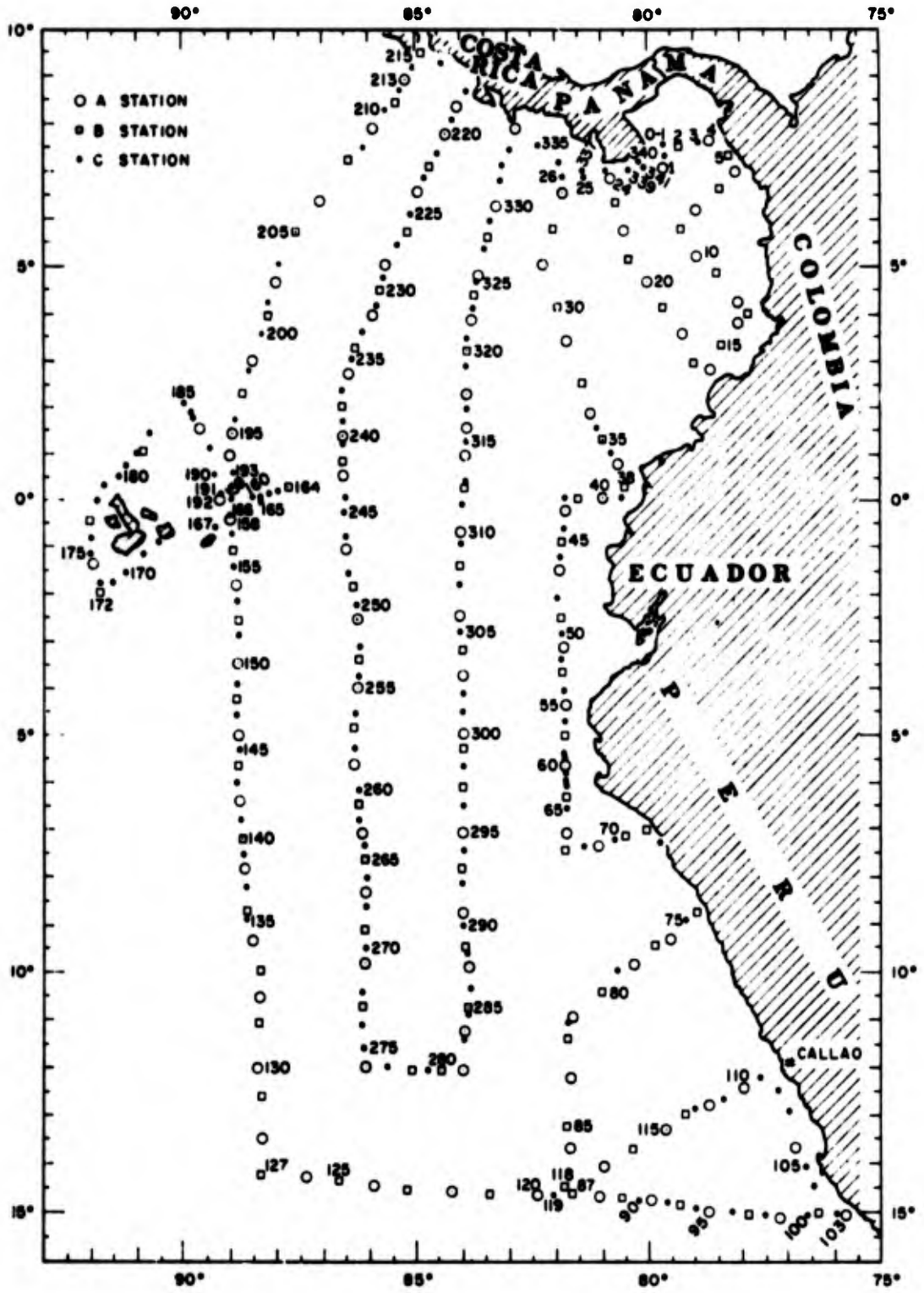

Figure 1. Stations of the R/V ALAMINOS EASTROPAC Studies; A stations (0-1000 m), B stations (0-500 m), C stations (0-300 m).

most of the flow passed in and out of the region on the west and the south. Consequently, vertical sections (of thermosteric anomaly and dissolved oxygen concentration) along the western and southern boundaries of the region permit the description and identification of the important currents entering and leaving the region. The water column structure and characteristics of these important currents are illustrated by means of station curves (T-Z, T-O_2, and T-S curves) for selected stations.

In order to show the interrelationships among the currents, quasi-horizontal circulation patterns over the interior of the region are interpreted from the distributions of acceleration potential and water characteristics (dissolved oxygen concentration and salinity) at surfaces of constant values of thermosteric anomaly. This method of obtaining the circulation pattern at isanosteric surfaces is termed isanosteric analysis and is patterned after the isentropic analysis of Montgomery (1938). The method is based upon the assumption that mixing and water movements are largely constrained to surfaces of constant thermosteric anomaly.

The geostrophic velocity at isanosteric surfaces is proportional to the gradient of acceleration potential at any given latitude. The dissolved oxygen concentration and salinity are water characteristics, and their distributions at isanosteric surfaces

are used to follow the movements of water. The value of isanosteric analysis in obtaining the circulation pattern arises from the confirmation among these different distributions of acceleration potential and water characteristics at each surface.

The isanosteric surfaces chosen for this study correspond to δ_T = 120, 160, 200, and 280 cl/t. They are chosen on the basis of results in the vertical sections and station curves, and of previous studies of the region.

To show further interrelationships among the currents and to indicate their continuity of flow, volume transports are presented.

Previous Studies

Perhaps the first evidence that water from the Equatorial Undercurrent extends east of the Galapagos Islands was presented by Montgomery and Stroup (1962). They found that the Equatorial Undercurrent maintained a volume transport maximum near 13°C (near 180 cl/t) and that the large thickness of the 13°C Water extended east of the Galapagos Islands to the coast of South America. The way in which the Undercurrent extended east of the Islands was not clear. Montgomery (1962), in a summary of observations about the Undercurrent east of the Islands, concluded that the

eastward motion was usually weak or absent there. The combined previous evidence led Wyrtki (1966) to believe that the Equatorial Undercurrent disintegrates west of the Galapagos Islands and that its transport spreads both north and south of the Islands, with some of the water extending to the upwelling regions off northern Peru.

Knauss (1966), in his discussion of the Equatorial Undercurrent east of the Galapagos Islands, reported direct current measurements, which showed eastward flow passing north of the Islands and extending as far east as 87°W. However, he did not find eastward flow south of the Islands, although the high oxygen and high salinity found there suggested to him that water from the Equatorial Undercurrent did penetrate into that region on some occasions.

Yoshida (1967), on theoretical grounds, found that the Equatorial Undercurrent divides west of the Galapagos Islands, with transport on the south extending to the coast of Peru to feed the Peru-Chile Undercurrent.

Tsuchiya (1968), in an isanosteric analysis of selected data for the intertropical Pacific Ocean, discussed the Equatorial Undercurrent in terms of its high oxygen concentration. At 160 cl/t, an equatorial band of high oxygen extended north of the Galapagos Islands and east to the coast. At 200 cl/t, the high oxygen band

extended through the Islands along the equator to about 85°W. Tsuchiya interpreted these bands of high oxygen to indicate that the Equatorial Undercurrent water extended east of the Galapagos Islands.

Cochrane and Zuta (1969), in another analysis of the R/V ALAMINOS data, showed two nearly parallel bands of eastward flow indicated in the mass structure and by two cores of high oxygen concentration near 2°N and 2°S. The bands passed on each side of the Galapagos Islands and extended nearly to the coast of South America. This suggested to them that the Equatorial Undercurrent split west of the Galapagos Islands into two branches (bands) of eastward flow.

The South Equatorial Countercurrent was noted by Reid (1959), on the basis of geostrophic considerations, as a subsurface eastward flow along 10°S. A similar current was identified by Wooster (1961) in a STEP-I meridional section at 95°W. He found eastward flow between 5° and 8°S with a maximum speed near the 160 cl/t isanosteric surface. The flow was associated with high oxygen. Combining the results of many cruises, Reid (1965) provided evidence that at 125 cl/t the South Equatorial Countercurrent extends across the entire Pacific Ocean near 10°S.

Wyrtki (1963) prepared subsurface geopotential topographies

from STEP-I data, which showed the South Equatorial Countercurrent extending east from 95°W to 86°W. There, the current turned back to form westward flow rather than extending to the coast. In this regard, his interpretation differed from those of Reid (1965), Tsuchiya (1968), and Cochrane and Zuta (1969). Reid's (1965) map of acceleration potential at the 125 cl/t surface depicted the South Equatorial Countercurrent extending to the coast of Peru near 13°S. Tsuchiya (1968) obtained similar results in his map of acceleration potential at the 160 cl/t surface. Cochrane and Zuta (1969) suggested that the South Equatorial Countercurrent supplied water to the Peru-Chile Undercurrent.

The Peru-Chile Undercurrent was first measured directly with the use of parachute drogues by Wooster and Gilmartin (1961) during the STEP-I Expedition. Previously, Gunther (1936) had noted that such a current would explain the high salinity and low oxygen core extending south along the coasts of Peru and Chile. Wooster and Gilmartin (1961) found similar properties associated with the Undercurrent and, in addition, found a maximum geostrophic speed near the 160 cl/t surface.

In Wyrtki's (1963) analysis of the STEP-I data, the southward flows noted by Wooster and Gilmartin (1961) were interpreted as two separate currents; a Peru-Chile Undercurrent immediately

adjacent to the coast and a Peru Countercurrent nearly 200 miles off the coast. The latter flow prevented transport of the South Equatorial Countercurrent from extending to the coast.

The name Chile Current was suggested by Wooster (1968) in reference to the northward current along the coast of Chile and southern Peru. Actually, he discerned two separate northward flows in echelon along the coast of South America. The Chile Current flows northward along the coast of Chile to about 20°S, where it turns seaward. Near there, what Wooster called the Peru Current forms closer to the coast. It is supplied with water from the west, and flows north to approximately 5°S, where it turns seaward.

Data

Data taken by the R/V ALAMINOS during the EASTROPAC studies are of two kinds: serial data taken with Nansen bottles and paired reversing thermometers, and continuous recordings of temperature, salinity, and depth made possible by an *in situ* instrument known as the STD. During the cruise, three types of stations were made: A and B stations, where both serial observations and STD measurements were taken to depths of at least 1000 m and 500 m, respectively; C stations, where only STD measurements

were taken to a depth of 300 m. The positions of these stations are shown in figure 1.

The water samples from the Nansen bottles were analysed for dissolved oxygen concentration by the Winkler method as modified by Carpenter (1965) and for salinity by the University of Washington conductive salinometer. On a few stations, salinity was determined by an I.M.E. (Industrial Manufacturing Engineers) inductance salinometer. The Nansen bottle samples, taken in the thermocline, were not analysed for salinity because the STD salinity was to be used there. Unfortunately, the STD salinity sensor has been found to give unreliable values in a strong thermocline.

In this study, only A and B stations are used, since C stations did not extend down to the reference level (500 m). Of the two different kinds of collected data, the STD was continuous, but the serial data more accurate. Therefore, this study relies on serial data almost exclusively, except for some salinity values in the thermocline. There, STD salinity values are used in the absence of Nansen bottle salinities. Where possible, these STD values are correlated with available Nansen bottle salinities in the immediate area. The salinity values in the thermocline are estimated to be accurate to within $\pm 0.03‰$.

Procedure

The vertical sections of thermosteric anomaly and dissolved oxygen concentration to a depth of 480 m were constructed from the station curves. In constructing the station curves, values of depth, dissolved oxygen concentration, and salinity were plotted against a common abscissa of temperature (on paper with pre-printed isopleths of thermosteric anomaly). Smoothed curves were drawn through the points to form T-Z, T-O_2, and T-S curves.

To construct the distribution of properties on isanosteric surfaces, the depth, dissolved oxygen concentration, and salinity were read from the station curves for values of constant thermosteric anomaly; at 10 cl/t intervals from 100 to 200 cl/t and at 20 cl/t intervals from 200 to 300 cl/t.

The acceleration potential (Y) was determined by an expression similar to that given by Montgomery and Stroup (1962):

$$Y - Y_o = \int_{\delta_{T_o}}^{\delta_T} p \, d\delta_T + p_o \, \delta_{T_o} \quad ,$$

where δ_{T_o} is the thermosteric anomaly of the reference pressure p_o. This expression differs from that of Montgomery and Stroup (1962), with the thermosteric anomaly used in place of the steric

volume anomaly. This substitution is justified by Montgomery and Wooster (1954), who demonstrated that in the eastern Pacific Ocean the steric volume anomaly can be replaced by the thermosteric anomaly in computing geostrophic velocities without appreciable loss of accuracy. The reference pressure in this integration was taken at 500 db, since Wooster and Reid (1963) found little difference in the transports of the eastern Pacific Ocean using 500 db or 1000 db as a reference. The integration in the above expression was approximated numerically by the trapazoidal rule, with increments in thermosteric anomaly of 10 cl/t from 100 to 200 cl/t and of 20 cl/t from 200 to 300 cl/t.

The volume transport (T) between isanosteric surfaces was calculated from the profile of geostrophic velocity, as indicated in the following expression:

$$T = \left[\int_{\overline{z}_1}^{\overline{z}_2} V_g \, dz \right] \cdot L \quad ,$$

where V_g is the geostrophic velocity, L is the distance between stations, and $\overline{z}$ is the average depth of the isanosteric surface, the average being taken over both stations involved in calculating the geostrophic velocity. The integration was approximated numerically by the trapazoidal rule, with increments in depth corresponding to thermosteric anomaly

increments of 20 cl/t from 120 to 200 cl/t and of 40 cl/t from 200 to 280 cl/t.

CHAPTER II

VERTICAL STRUCTURE

The vertical sections along the western and southern boundaries of the region are used to describe and identify the important subsurface flows which passed into and out of the region. The station curves (T-Z, T-O_2, and T-S curves) for selected stations illustrate the water column structure of the important flows and indicate possible interrelationships among the flows.

Vertical Sections

Figure 2(a) shows the distribution of thermosteric anomaly in the vertical section along the western edge of the region at approximately 89°W. Figure 2(b) shows the corresponding distribution of oxygen. Figure 3(a) shows the distribution of thermosteric anomaly in the vertical section along the southern edge at approximately 15°S and figure 3(b) the corresponding distribution of oxygen.

In the meridional section, the eastward flows are of special interest. Between 3° and 4°S, the isanosteres from 120 to 300 cl/t sloped upward away from the equator. This upslope indicates geostrophic eastward flow with speed increasing upwards. From 170 to 190 cl/t, the slope of the isanosteres decreased considerably.

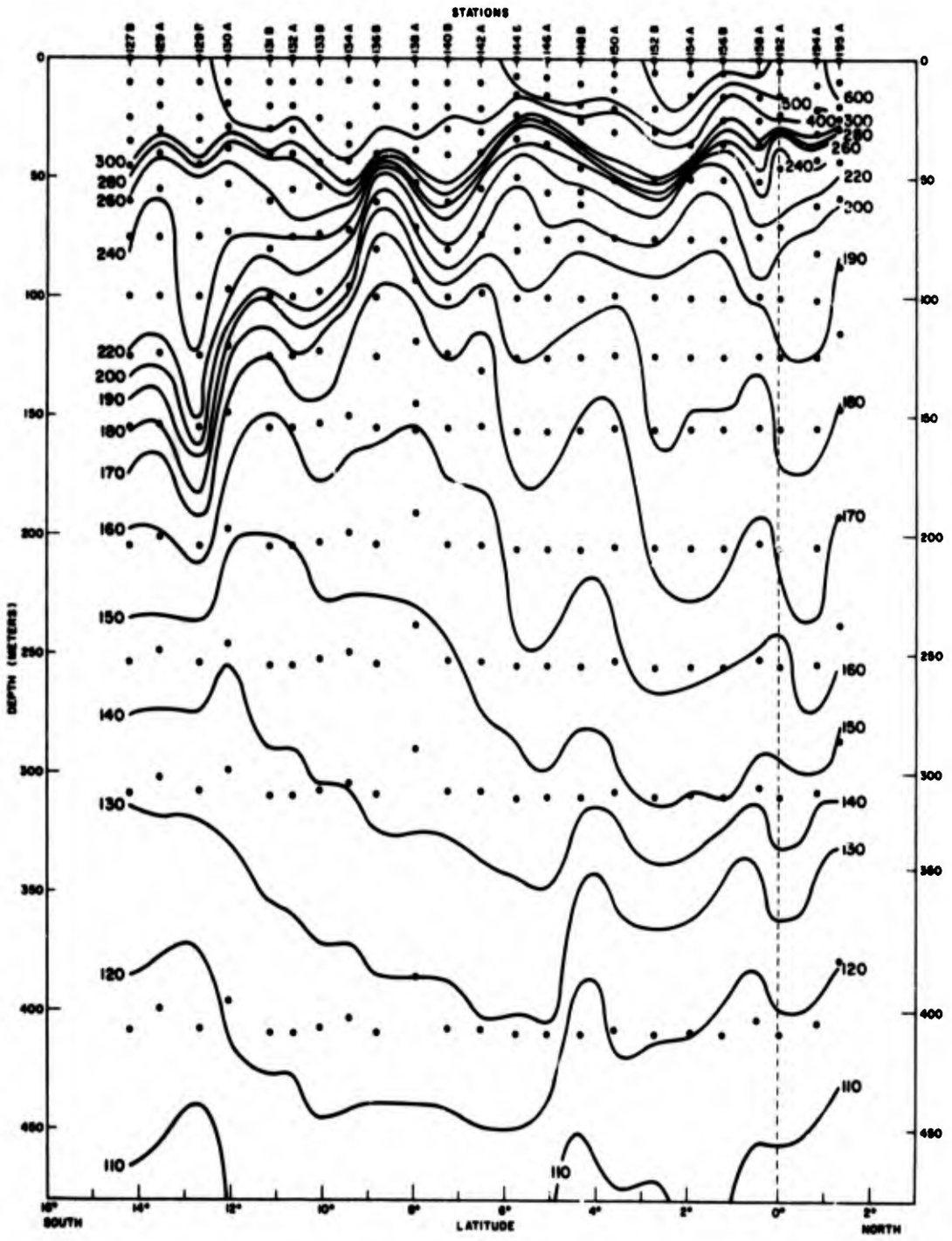

Figure 2(a). Thermosteric anomaly (centiliters per ton) along approximately 89°W from 2°N to 15°S.

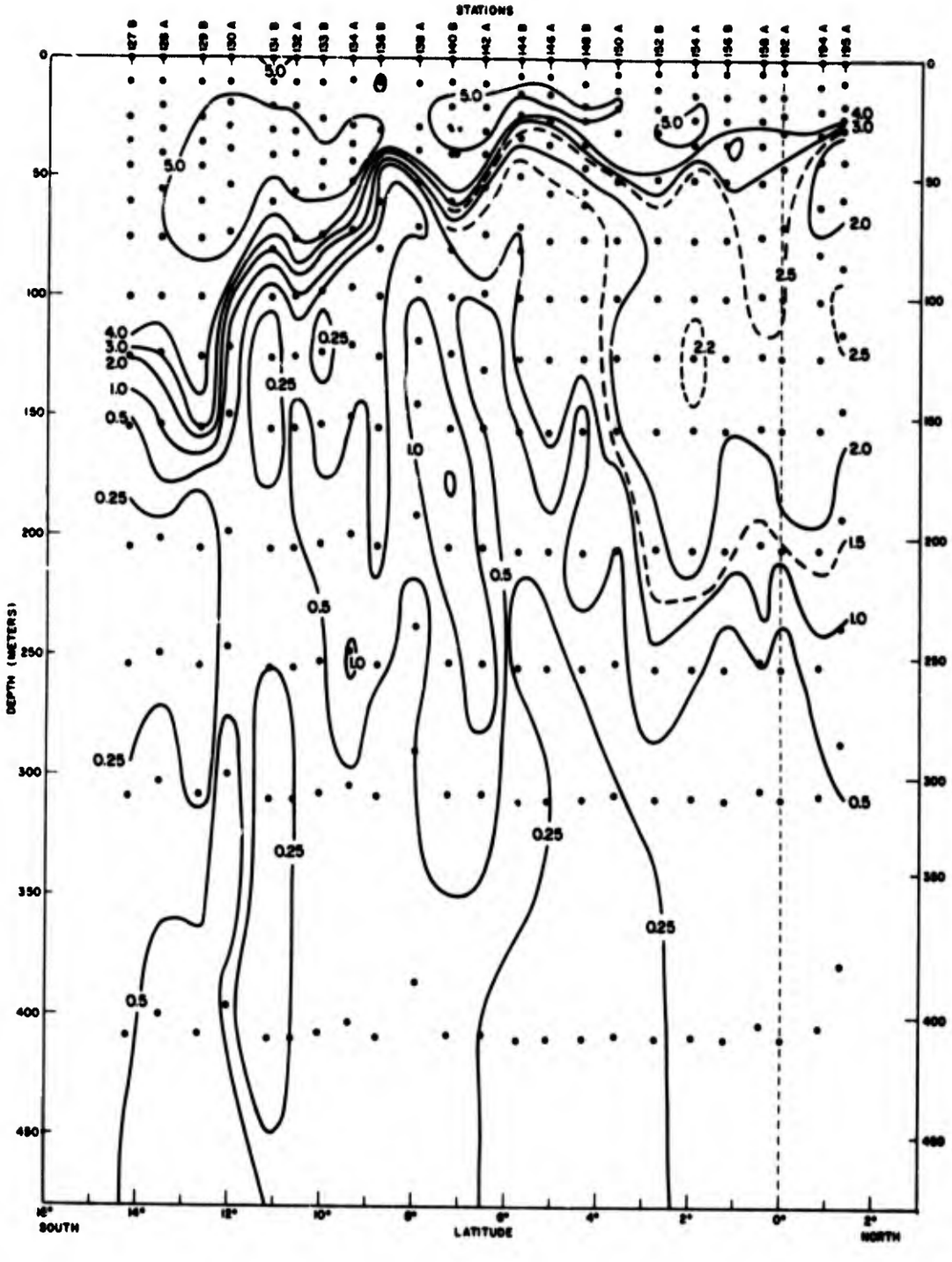

Figure 2(b). Oxygen (milliliters per liter) along approximately 89°W from 2°N to 15°S.

As a result, the isanosteres near 3°S spread apart. Also near 3°S, as figure 2(b) shows, a core of high oxygen (>2.00 ml/l) was present from about 170 to 190 cl/t. Tsuchiya (1968) showed similar high oxygen and large thickness associated with the Equatorial Undercurrent west of the Galapagos Islands. The eastward flow was the apparent eastward extension of the Equatorial Undercurrent passing south of the Galapagos Islands, which was noted by Cochrane and Zuta (1969). Hereafter, this flow will be called the south branch of the Equatorial Undercurrent.

Another eastward flow was indicated between 6° and 13°S, where the 120 cl/t isanostere sloped upward away from the equator. The upslope extended only to 11°S at 160 cl/t and to 9°S at 200 cl/t. The maximum upslope lay between 6° and 8°S from 150 to 180 cl/t and was accompanied by a spreading of the isanosteres near 7°S. Between 7° and 8°S, there was a narrow core of high oxygen (>1.00 ml/l). Similar upslopes between 5° and 8°S, associated with high oxygen values, were reported by Wooster (1961), who considered these features to be indicative of the South Equatorial Countercurrent.

In the zone from 4° to 6°S, between the two eastward flows, the isanosteres from 120 cl/t to 220 cl/t sloped down toward the south. Such slopes indicate westward flow. The flow was accompanied by relatively low oxygen (<0.5 ml/l).

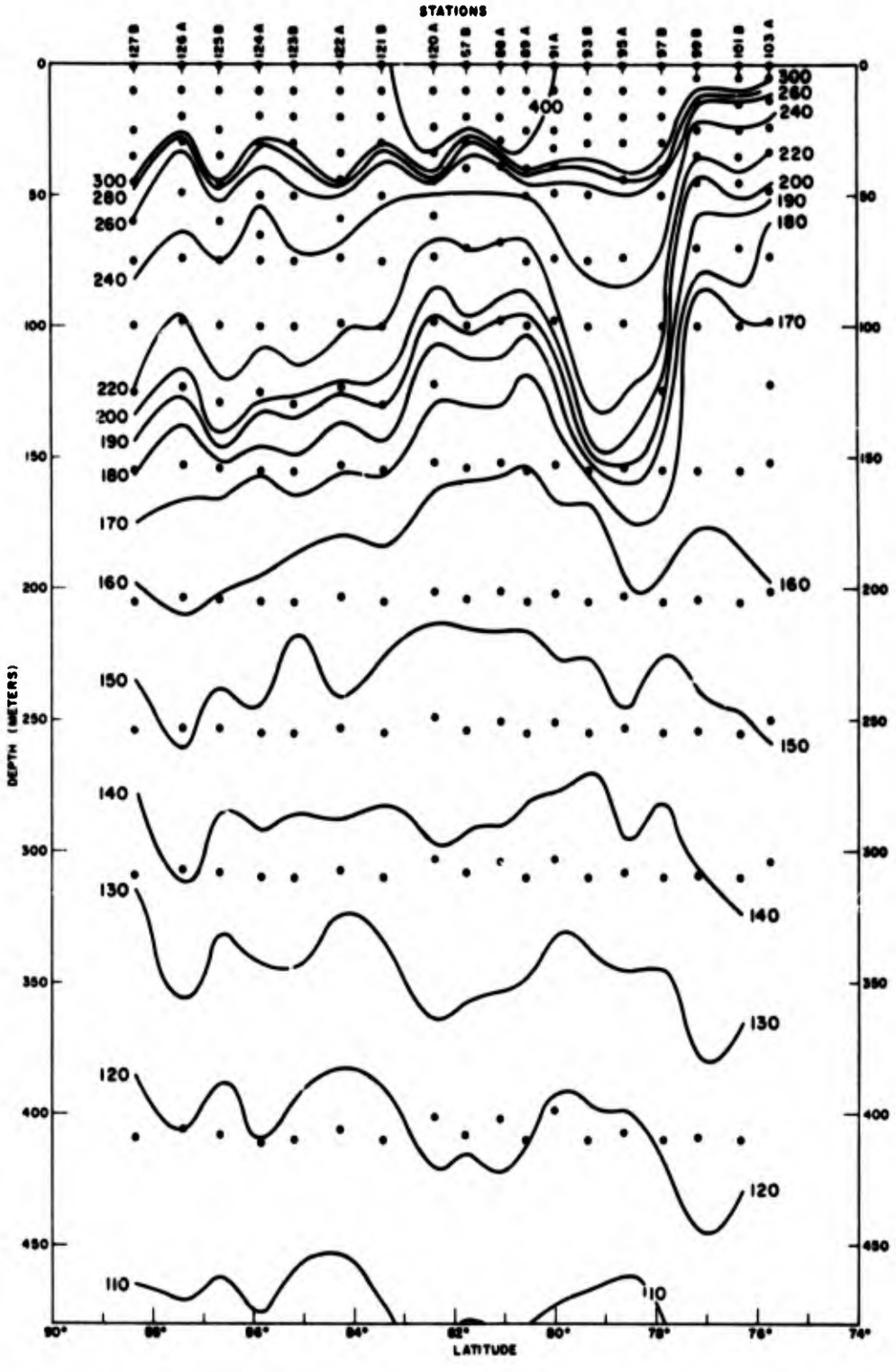

Figure 3(a). Thermosteric anomaly (centiliters per ton) along approximately 15°S from 76°W to 89°W.

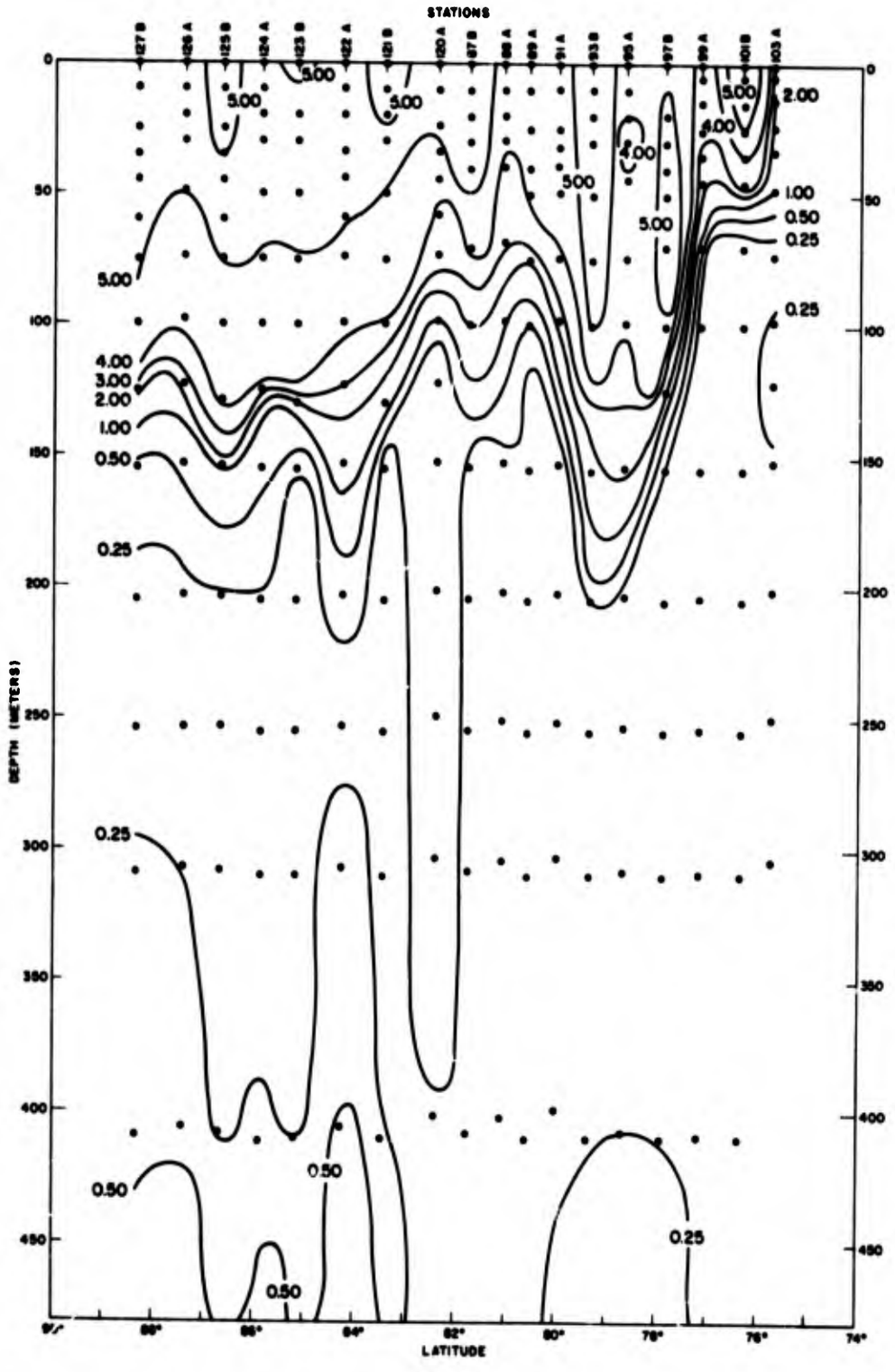

Figure 3(b) Oxygen (milliliters per liter) along approximately 15°S from 76°W to 89°W.

Another westward flow was indicated at the southern boundary of the South Equatorial Countercurrent. In view of Wooster's (1969) description of the Chile Current, this flow was probably the westward extension of that current as it turned seaward from the coast. The flow carried high oxygen (> 2.00 ml/l) above 160 cl/t, which agrees with the high oxygen that Tsuchiya found in a similar current.

Between 76° and 78°W in the zonal section [figures 3(a) and 3(b)], the isanosteres from 120 to 180 cl/t sloped upward away from the coast to a ridge near 78°W. This upslope indicates southward geostrophic flow with a maximum speed near 180 cl/t. From the oxygen section [figure 3(b)], the southward flow is seen to carry water of low concentration (< 0.25 ml/l) in the layers below 180 cl/t. This subsurface flow of water of low oxygen appears to be the Peru-Chile Undercurrent, described by Wooster and Gilmartin (1961).

Between 77° and 79°W, the isanosteres above 160 cl/t, which sloped down away from the coast, indicate northward flow. This was accompanied by high oxygen (> 2.00 ml/l). The northward flow was probably an offshoot of the Chile Current, the westward extension of which appeared in the meridional section. The southward flow between 79° and 80°W was also of high oxygen and

probably represented a return of the preceding northward flow. The westward extension of the Chile Current is indicated farther west on this section.

In summary, it may be said that the sections show two eastward flows, the south branch of the Equatorial Undercurrent and the South Equatorial Countercurrent entering the region from the west; the two flows were separated by a westward flow near 5°S. The Peru-Chile Undercurrent traveled south out of the region next to the coast and an offshoot of the Chile Current extending north along its west side. The westward extension of the Chile Current was found to pass through the southern part of the region toward the northwest.

Station Curves

The water column structure of the south branch of the Equatorial Undercurrent is represented by the station curves for station 150, shown in figure 4. In the T-Z curve between 150 and 190 cl/t, a layer of small vertical temperature gradient is shown. Such a layer is called a thermostad following Seitz (1967). The thick layer between 150 and 190 cl/t, because it is typical of the equatorial regions, may be called the equatorial thermostad. This feature of the Undercurrent is represented in the meridional sections by

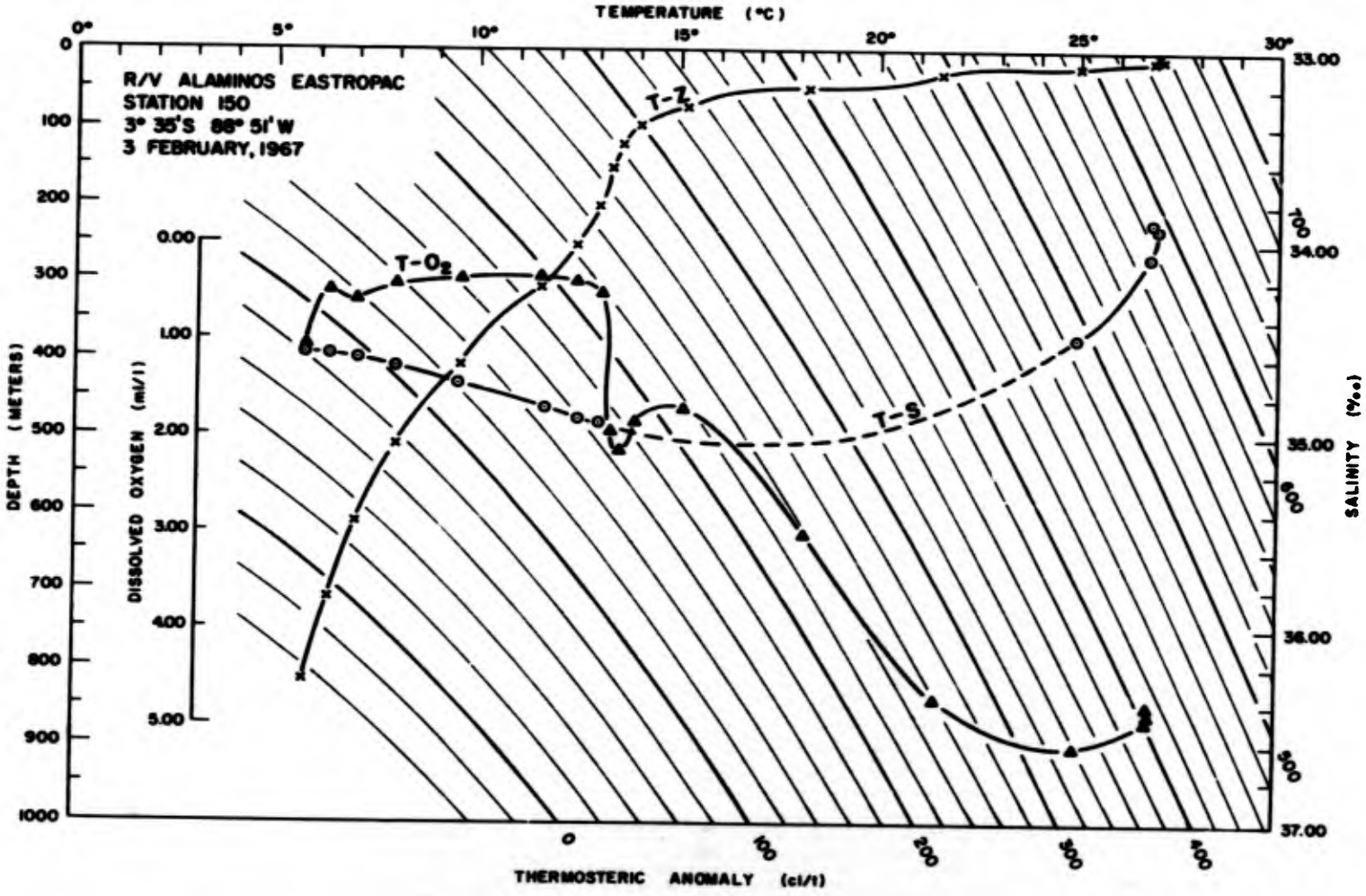

Figure 4. Temperature (°C) plotted against depth (m), salinity (‰), and oxygen (ml/l) for station 150.

spreading of the isanosteres near 3°S. Montgomery and Stroup (1962) and Tsuchiya (1968) showed a similar equatorial thermostad at stations near the equator, at 150°W and at 95°W, respectively. The T-O_2 curve displays a maximum (2.20 ml/l) in the oxygen concentration near 180 cl/t in the upper equatorial thermostad. Both above and below this feature, minimum oxygen values were found at 200 cl/t and 150 cl/t. Tsuchiya (1968) showed a similar oxygen maximum near 180 cl/t at the above mentioned equatorial station at 95°W.

The water column structure of the South Equatorial Countercurrent is represented by the station curves (figure 5) for station 140. In the T-Z curve, a thermostad was found between 120 and 180 cl/t, deeper and less distinct than that of the south branch of the Equatorial Undercurrent. The T-O_2 displays a strong oxygen maximum near 160 cl/t at the top of the thermostad. Both above and below this feature, oxygen minimum values were found near 180 cl/t and 120 cl/t.

The westward flow near 5°S had a water column structure represented by the station curves (figure 6) for station 146. In the T-Z curve, a thermostad was found between 140 and 200 cl/t. The T-O_2 curve exhibits two maxima below the surface layers, one at 190 cl/t and the other at 150 cl/t. The oxygen maximum at 190 cl/t

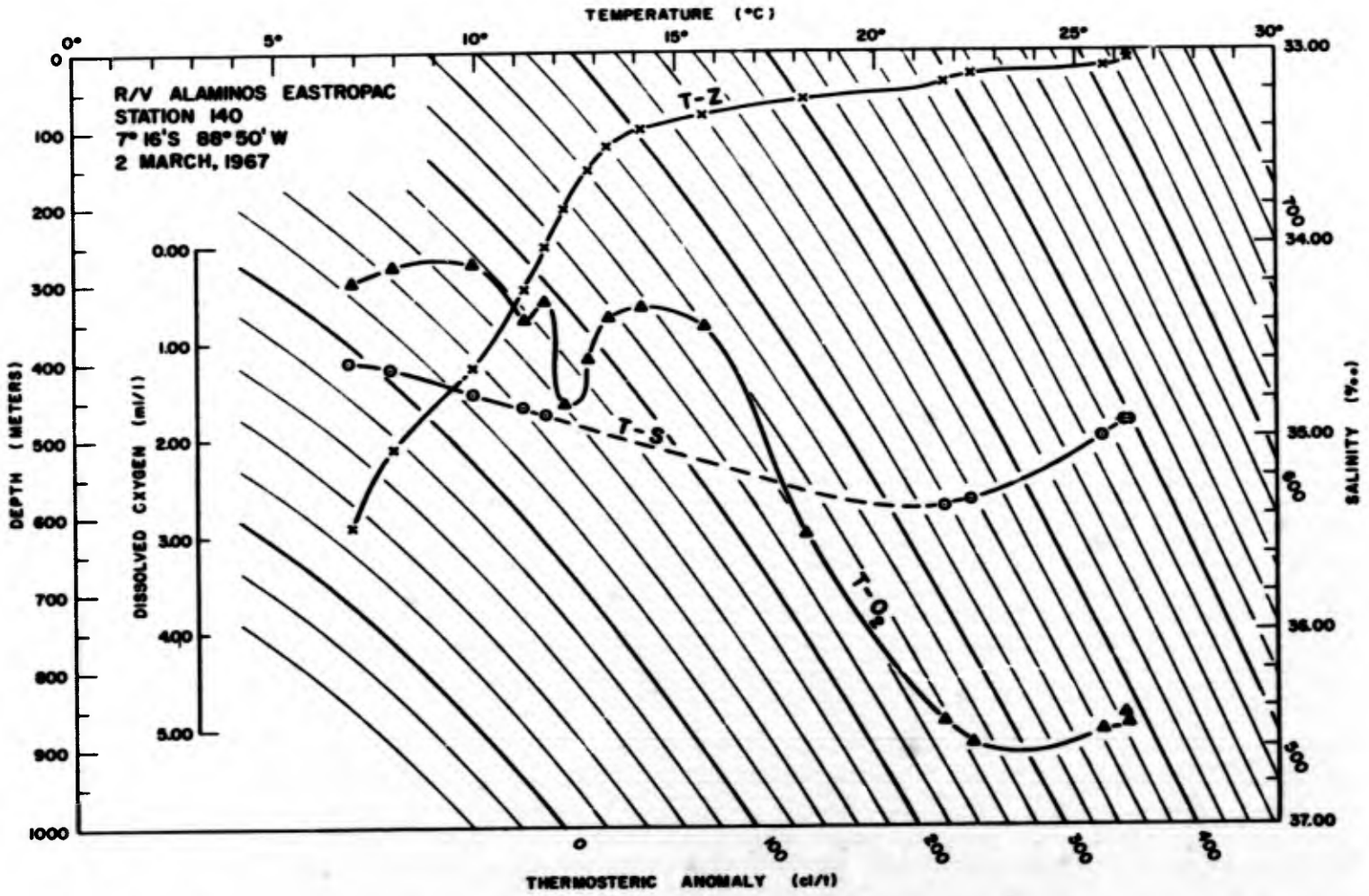

Figure 5. Temperature (°C) plotted against depth (m), salinity (‰), and oxygen (ml/l) for station 140.

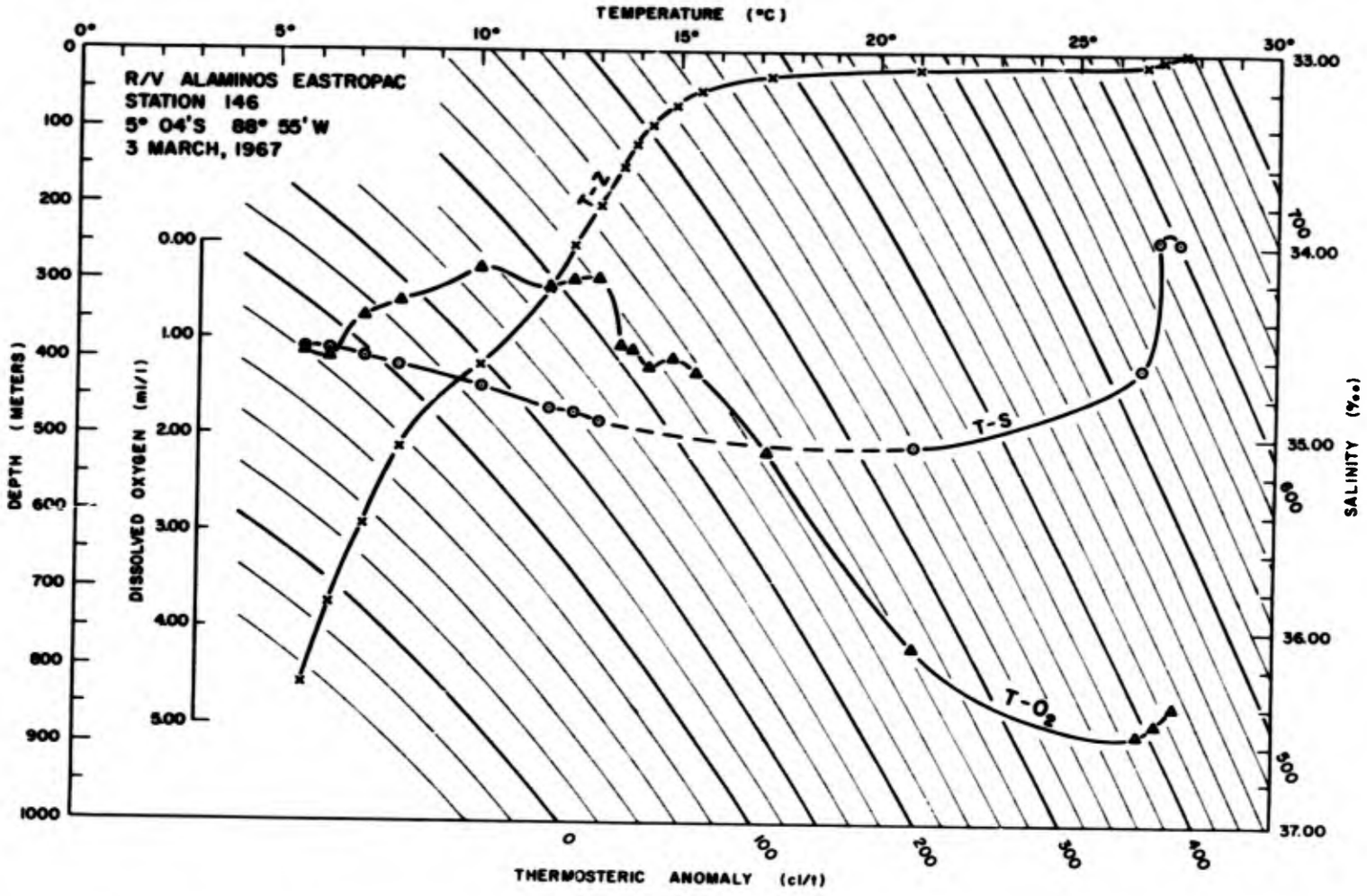

Figure 6. Temperature (°C) plotted against depth (m), salinity (‰), and oxygen (ml/l) for station 146.

suggests the presence of water from the south branch of the Equatorial Undercurrent. The oxygen maximum at 150 cl/t, together with the deep thermostad, suggests a contribution to the flow from the South Equatorial Countercurrent.

The water column structure of the offshoot of the Chile Current is represented by the station curves (figure 7) for station 95. In the T-S curve, a secondary salinity minimum was located near 200 cl/t at the base of the thermocline. In the $T\text{-}O_2$ curve, the rather high oxygen concentration of the upper layers decreased abruptly below the secondary salinity minimum.

The Peru-Chile Undercurrent had a water column structure represented by the station curves (figure 8) for station 77. The T-Z curve shows a thermostad between 160 and 190 cl/t. The $T\text{-}O_2$ curve displays the remnants of two minor maxima below the surface layer, one near 180 cl/t and the other near 160 cl/t. The oxygen maximum near 180 cl/t, together with the thermostad, suggests the presence of water from the south branch of the Equatorial Undercurrent. The oxygen maximum near 160 cl/t suggests the presence of water from the South Equatorial Countercurrent. The T-S relation exhibits a small secondary salinity minimum at 200 cl/t, which may be the result of an admixture of water from the offshoot of the Chile Current.

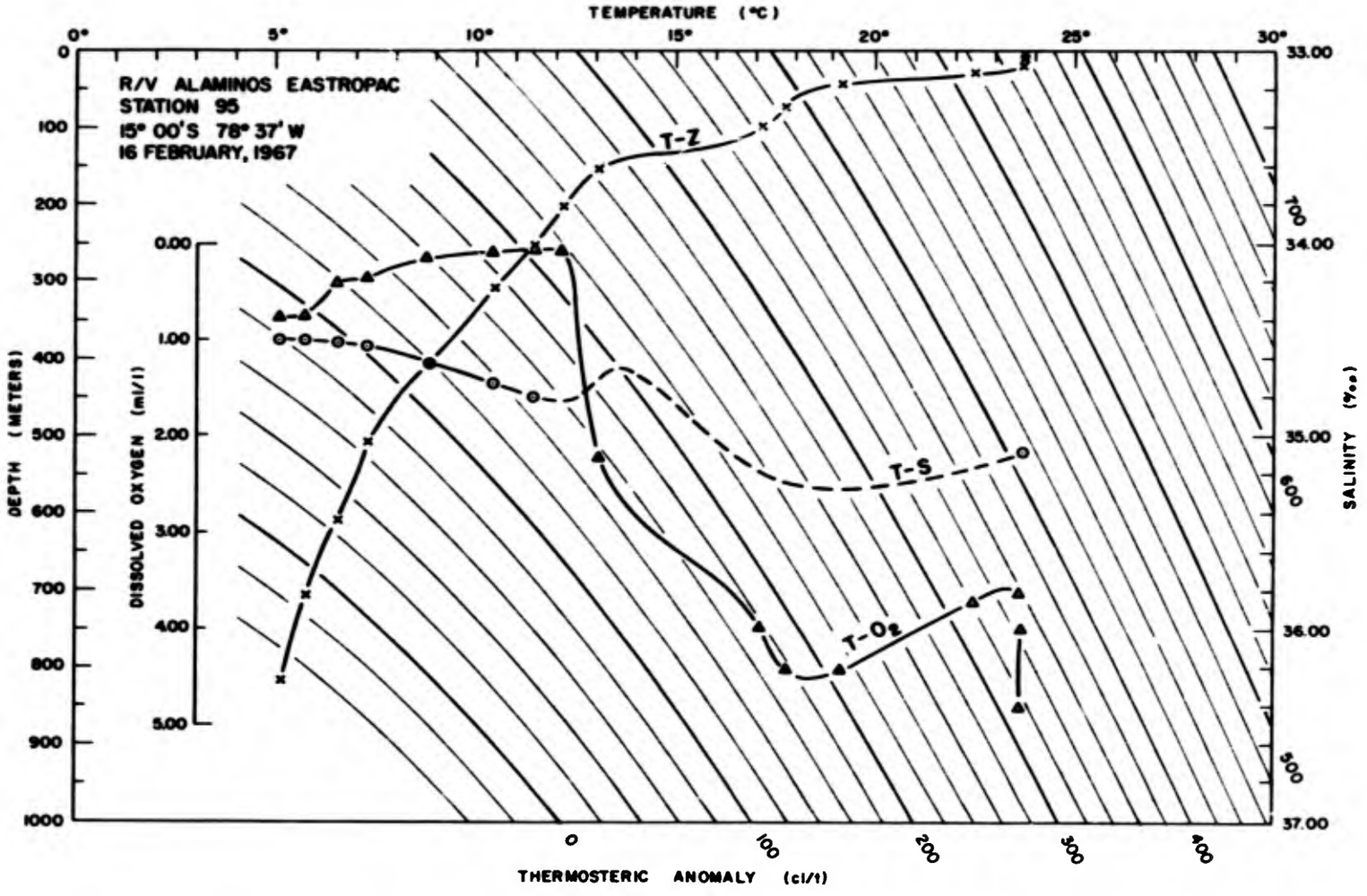

Figure 7. Temperature (°C) plotted against depth (m), salinity (‰), and oxygen (ml/l) for station 95.

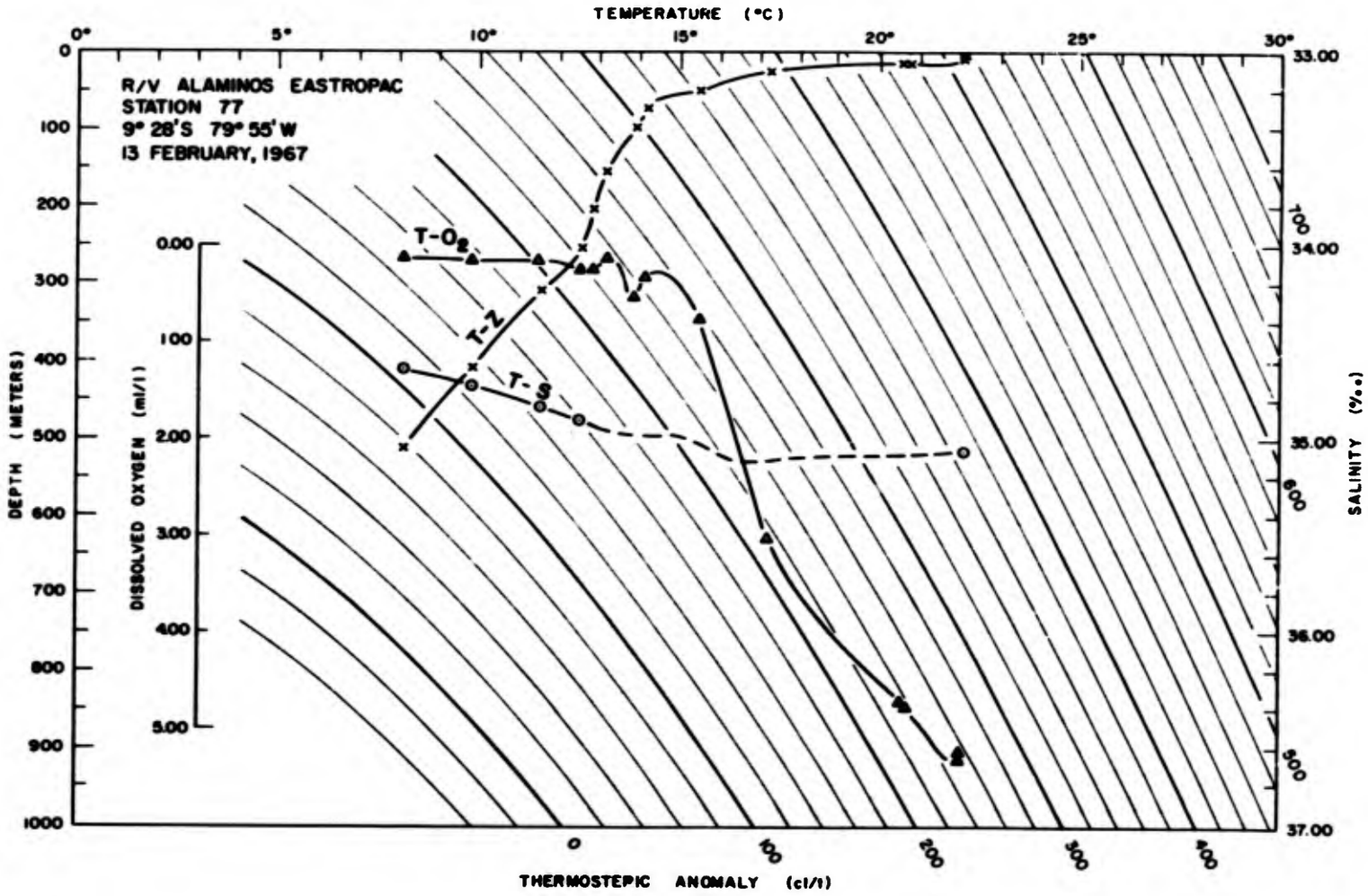

Figure 8. Temperature (°C) plotted against depth (m), salinity (‰), and oxygen (ml/l) for station 77.

CHAPTER III

DISTRIBUTION OF PROPERTIES ON ISANOSTERIC SURFACES

In order to follow the important currents within the region and to describe their interrelationships, the acceleration potential and water characteristics (dissolved oxygen concentration and salinity) are mapped at various isanosteric surfaces. The surfaces where δ_T = 120, 160, 200, and 280 cl/t are presented. The 160 and 200 cl/t surfaces turned out to be the most representative of the circulation patterns of the region. The 120 cl/t surface was near the reference pressure (500 db), while the 280 cl/t surface was within 50 m of the sea surface. In addition, the dissolved oxygen concentration at 180 cl/t and the thickness of the layer from 170 to 190 cl/t are given in order to show the thermostad and high oxygen core of the south branch of the Equatorial Undercurrent.

The 120 cl/t Surface

Figure 9(a) shows the topography of the 120 cl/t surface, which lay between 360 and 450 m in depth. At 3°S, a trough (>400 m) extended into the region from the west to the coast of Ecuador. The trough may have been an extension of an equatorial trough which Reid (1965) found in the 125 cl/t surface west of the Galapagos

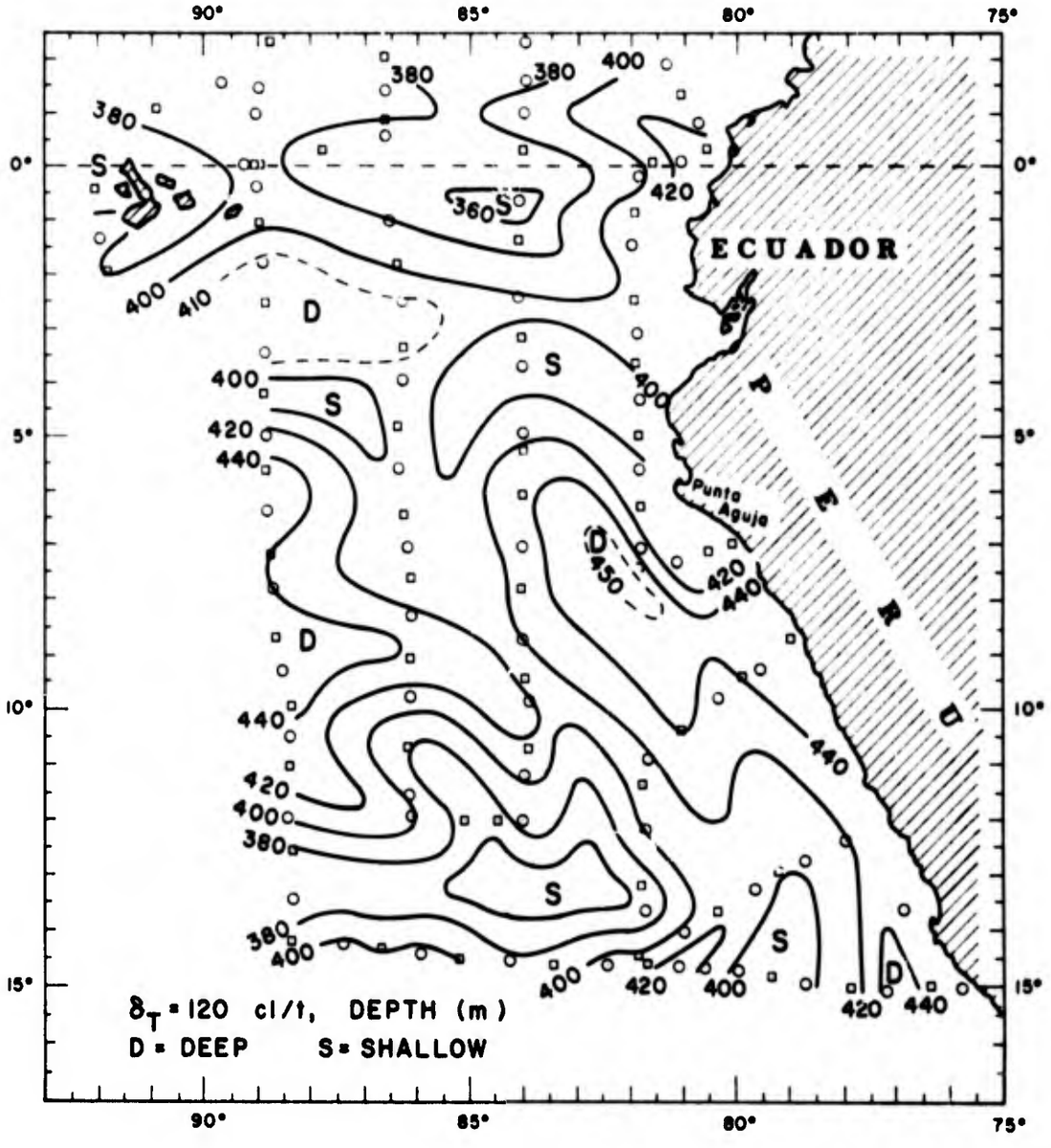

Figure 9(a). Depth (meters) of the surface where $\delta_T = 120$ cl/t.

Islands. Farther south between 7° and 12°S, another trough (>420 m) extended into the region to 84°W. South of the trough, the surface shoaled abruptly (<380 m) to form a ridge along 13°S. Reid (1965) noted a similar ridge in the 125 cl/t surface along the south edge of the South Equatorial Countercurrent. Next to the coast of Peru south of 9°S, the surface sloped upward from east to west, suggesting southward flow.

Figure 9(b) displays the acceleration potential at the 120 cl/t surface. Between 2° and 4°S, an eastward flow entered the region. Evidence from the meridional sections [figures 2(a) and 2(b)] indicates this flow to be the south branch of the Equatorial Undercurrent. It extended east to 83°W, although a considerable part of the flow turned north to join the westward flow nearer the equator. At 83°W, the eastward flow was joined by water from the vicinity of the equator; the combined flow turned southward and extended along the coast to approximately 5°S. There, most of the flow turned seaward and continued west along a meandering path out of the region near 5°S. A small portion of the westward flow turned south near 84°W, extended to about 10°S, and from there returned toward the coast.

Between 11° and 13°S, another eastward flow entered the region. Evidence from the meridional sections [figures 2(a) and 2(b)]

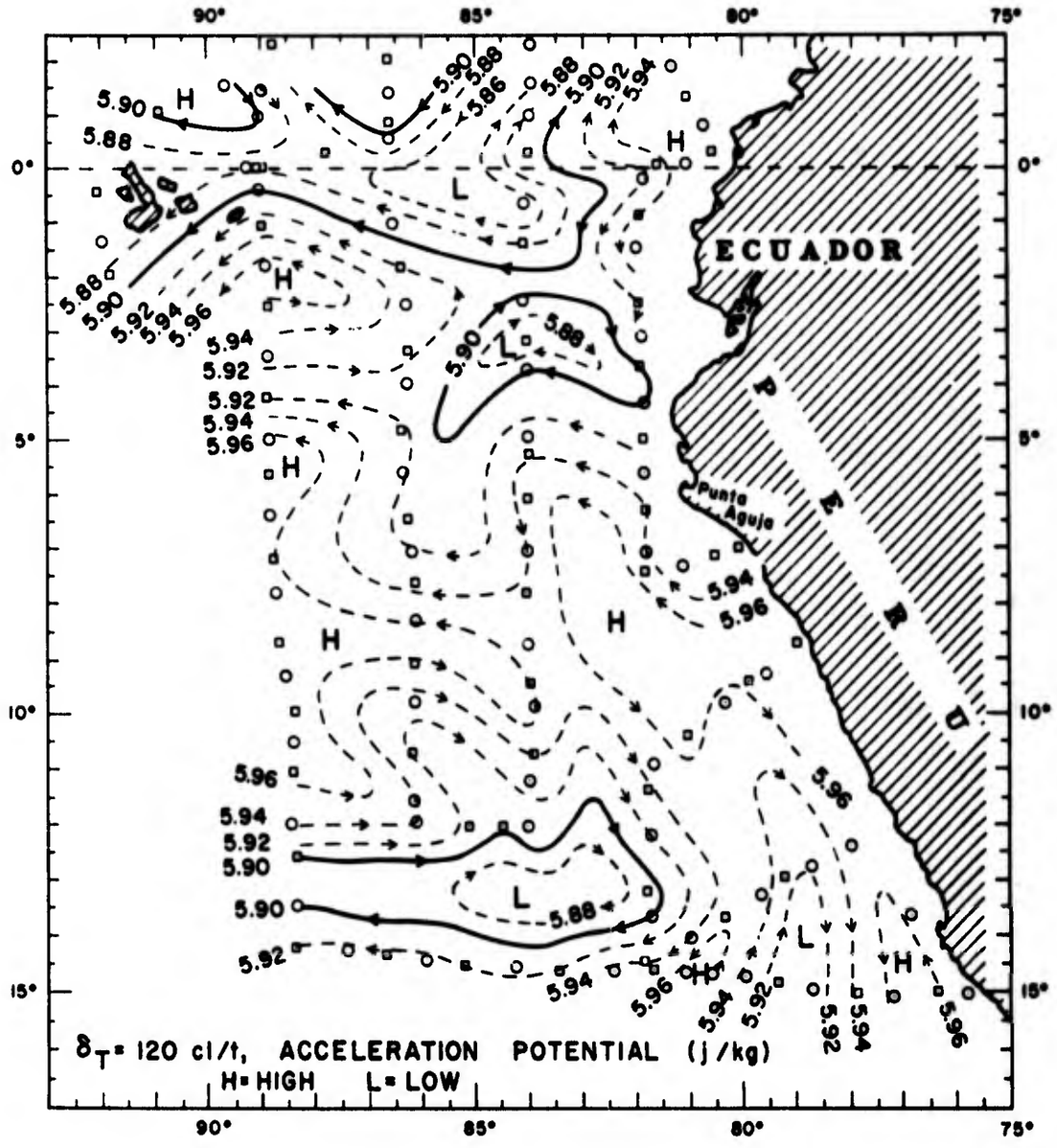

Figure 9(b). Acceleration potential (dynamic decimeters or joules per kilogram) relative to 500 decibars on the surface where $\delta_T = 120$ cl/t.

indicate this to be the South Equatorial Countercurrent. This current extended east to 84°W; there, some of the flow turned north to join the westward flow leaving the region at 5°S, while most of the flow turned southward, and then westward to form a cyclonic loop elongated along 13°S. This westward flow, south of 13°S, was the westward extension of the Chile Current shown in the meridional section [figure 2(a)].

Along the coast of Peru south of 10°S, a southward current was formed by flow that came in from the west. Near 12°S, the southward flow was augmented by water that had reached there by coming north along 80°W. The combined southward flow continued out of the region along 78°W. From the zonal sections [figures 3(a) and 3(b)], the current appeared to be the Peru-Chile Undercurrent observed by Wooster and Gilmartin (1961).

The northward flow along 80°W was characterized by relatively low salinity values [figure 9(d)]. Reid (1965) noted that low salinity is associated with a northward flow, which has been called the Chile Current by Wooster (1968). In view of Wooster's description of this current, the northward flow along 80°W appears to be an offshoot of the Chile Current.

Figure 9(c) shows the distribution of oxygen at the 120 cl/t surface. Near 2°S, a band of high oxygen (> 0.35 ml/l) extended

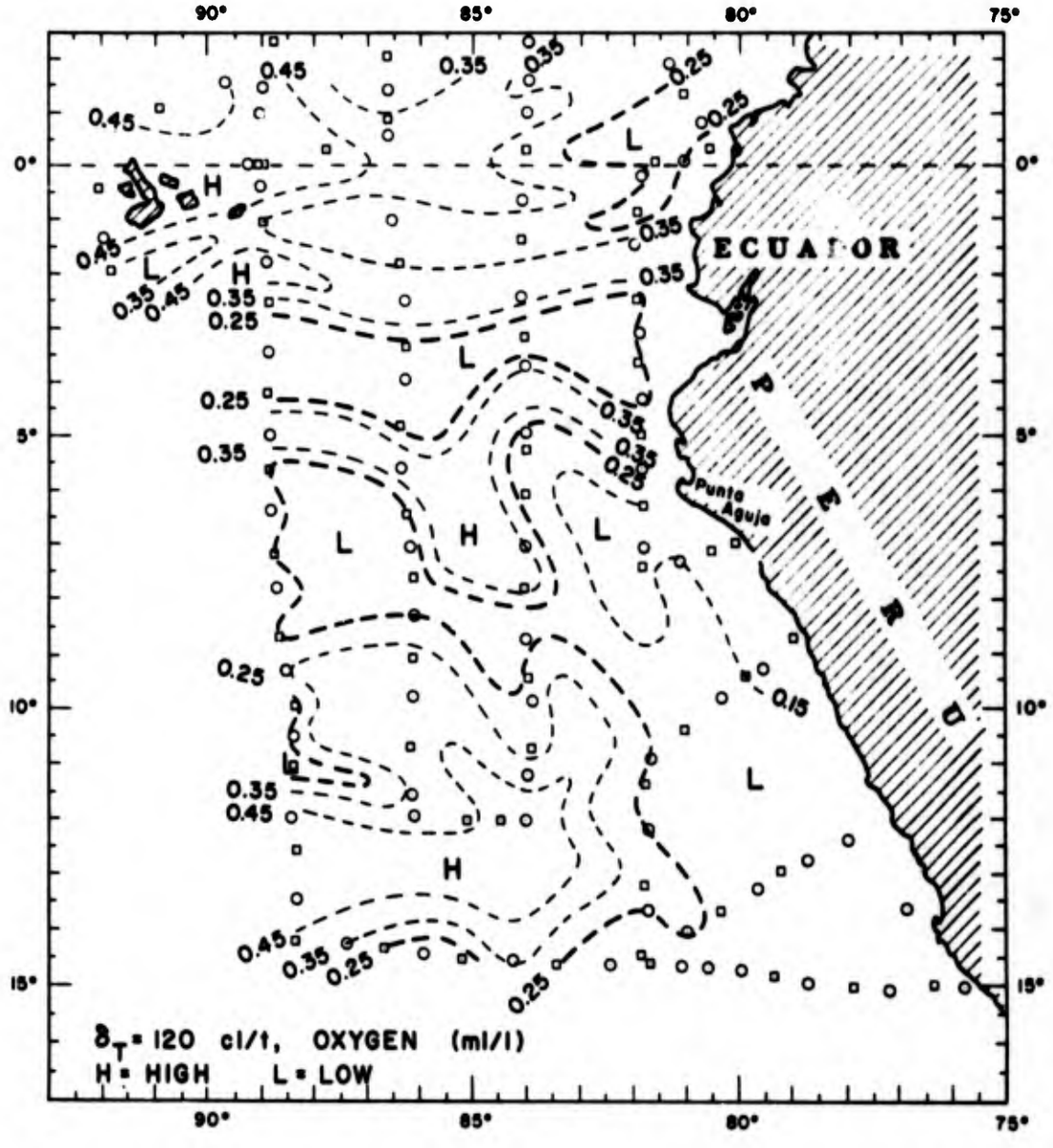

Figure 9(c). Oxygen (milliliters per liter) on the surface where δ_T = 120 cl/t.

along the northern part of the south branch of the Equatorial Undercurrent to the coast of Ecuador. At the coast, the high oxygen values apparently continued south to 5°S, where they turned west with the seaward flow near that latitude.

Between 12° and 14°S, a high oxygen tongue entered the region along the southern edge of the South Equatorial Countercurrent to 87°W. Between this high oxygen area and that near 5°S, a zone of low oxygen (< 0.25 ml/l) extended seaward from the coast of Peru. This location agrees to a large extent with Reid's (1965) position of the lowest oxygen values at the 125 cl/t surface.

Figure 9(d) exhibits the distribution of salinity at the 120 cl/t surface. Between 1° and 2°S, a band of high salinity (34.72 ‰) was situated along the northern part of the south branch of the Equatorial Undercurrent. This band appears to correspond to the high oxygen concentration along this same latitude. At the coast, the saline band apparently turned first to the south and then, at 5°S, to the west to extend out of the region with the westward flow near that latitude.

Between 10° and 12°S, high salinity (>34.70 ‰) extended into the region, as far east as 86°W, along the northern side of the South Equatorial Countercurrent. Reid (1965) also showed at 125 cl/t high salinity along the northern edge of the Countercurrent.

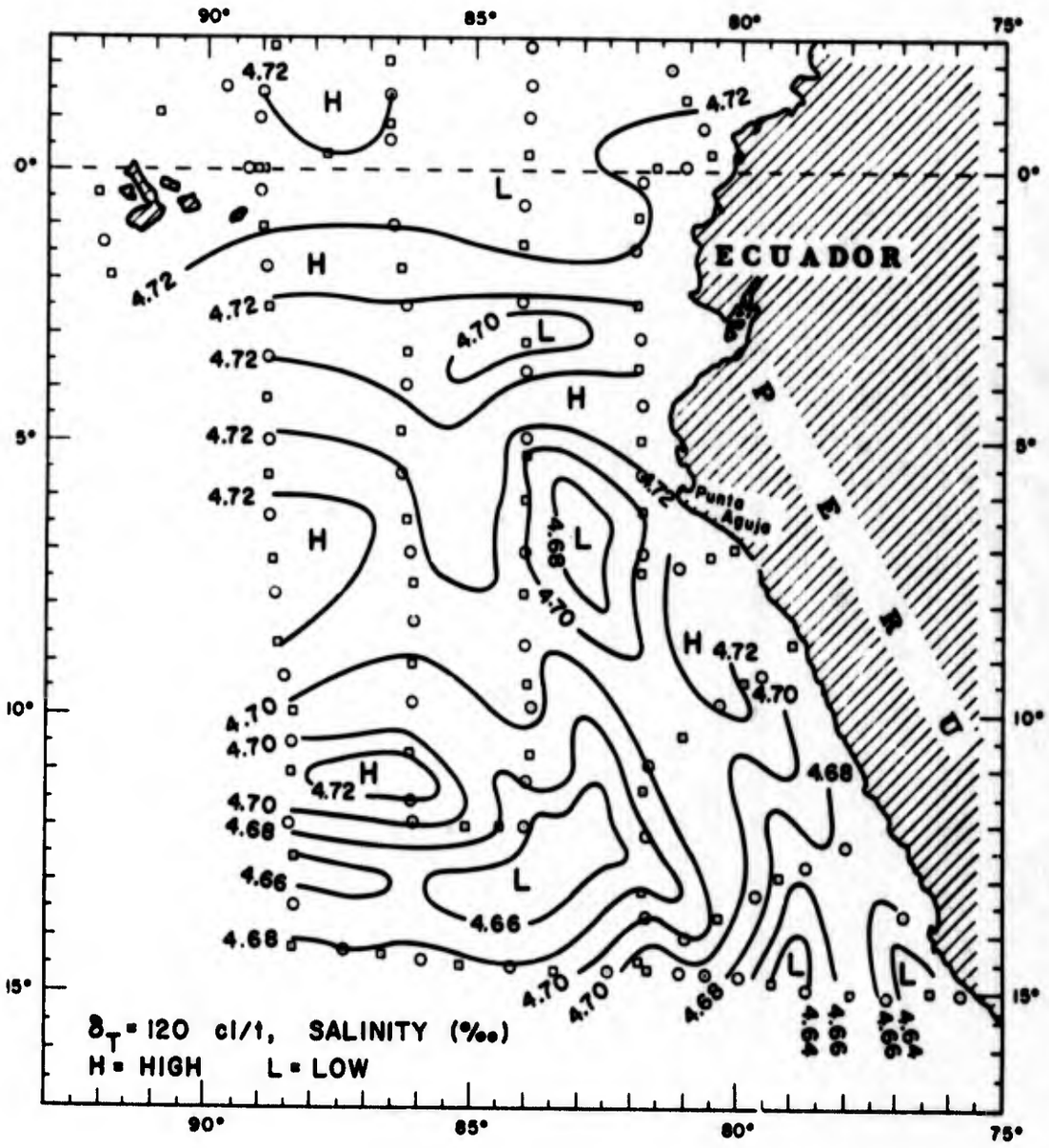

Figure 9(d). Salinity (‰) on the surface where $\delta_T = 120$ cl/t (add 30.00‰ to salinity values).

Between 12° and 14°S, low salinity water (< 34.68 ‰) extended east into the region to 82°W. It was nearly coincident with the high oxygen tongue at that same latitude and lay in the region between the South Equatorial Countercurrent and the westward extension of the Chile Current.

At 7°S next to the coast, a high salinity (34.72 ‰) tongue started south and extended as a ridge out of the region along 78°W. It was associated with the Peru-Chile Undercurrent. On its west side, a low salinity tongue (< 34.68 ‰) associated with the offshoot of the Chile Current, extended northward into the region to 11°S.

The 160 cl/t Surface

Figure 10(a) shows the 160 cl/t to lie between 140 and 300 m in depth. In comparison with the 120 cl/t surface, the topographic features at 160 cl/t were displaced northward. Two troughs appeared along the southern edge of the region and were associated with the westward extension of the Chile Current and related currents. The extension, as shown in the meridional sections [figures 2(a) and 2(b)], penetrated farther into the region at 160 cl/t than at 120 cl/t.

The acceleration potential at the 160 cl/t surface, shown in figure 10(b), indicates that the circulation pattern was similar to

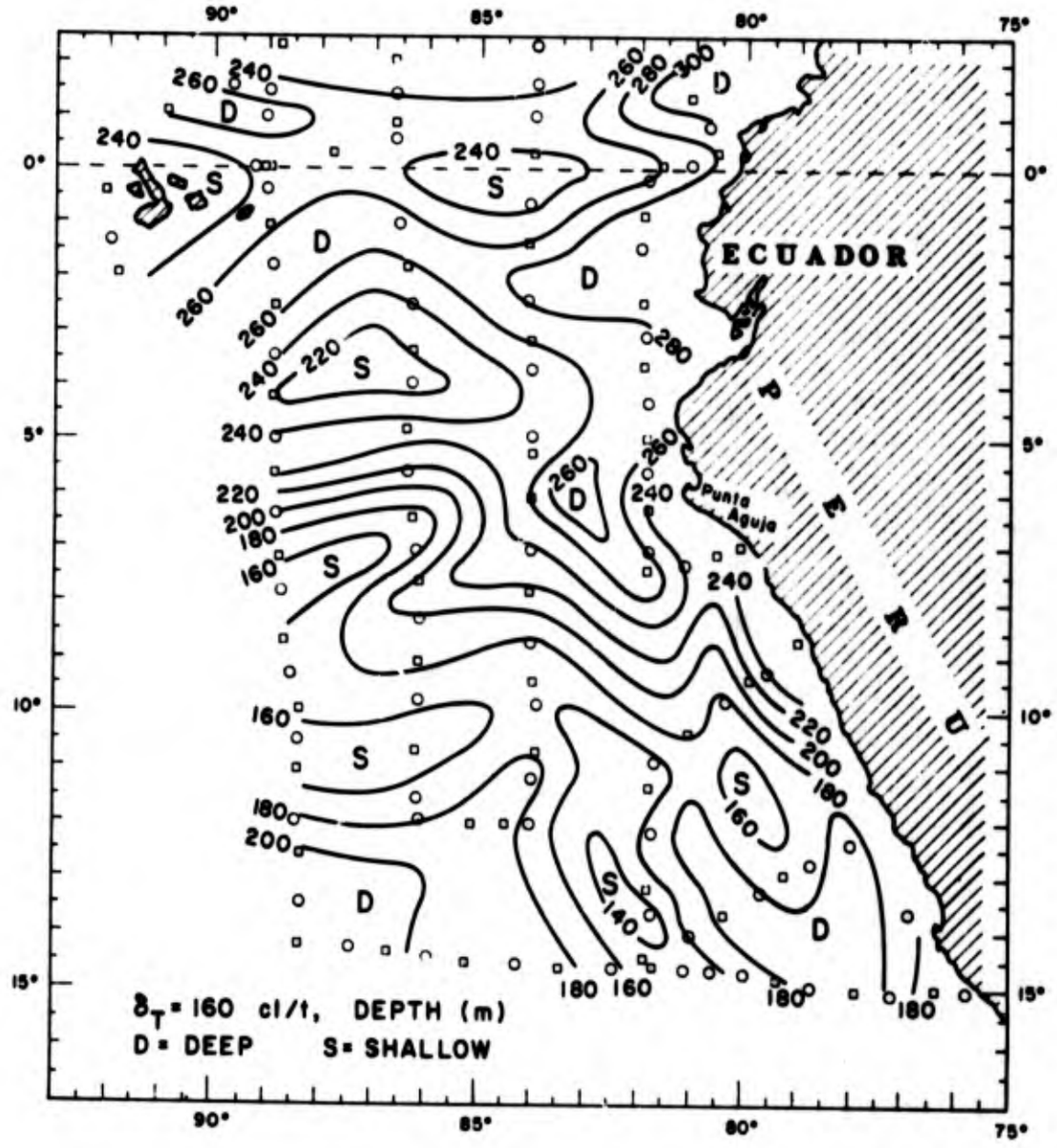

Figure 10(a). Depth (meters) of the surface where δ_T = 160 cl/t.

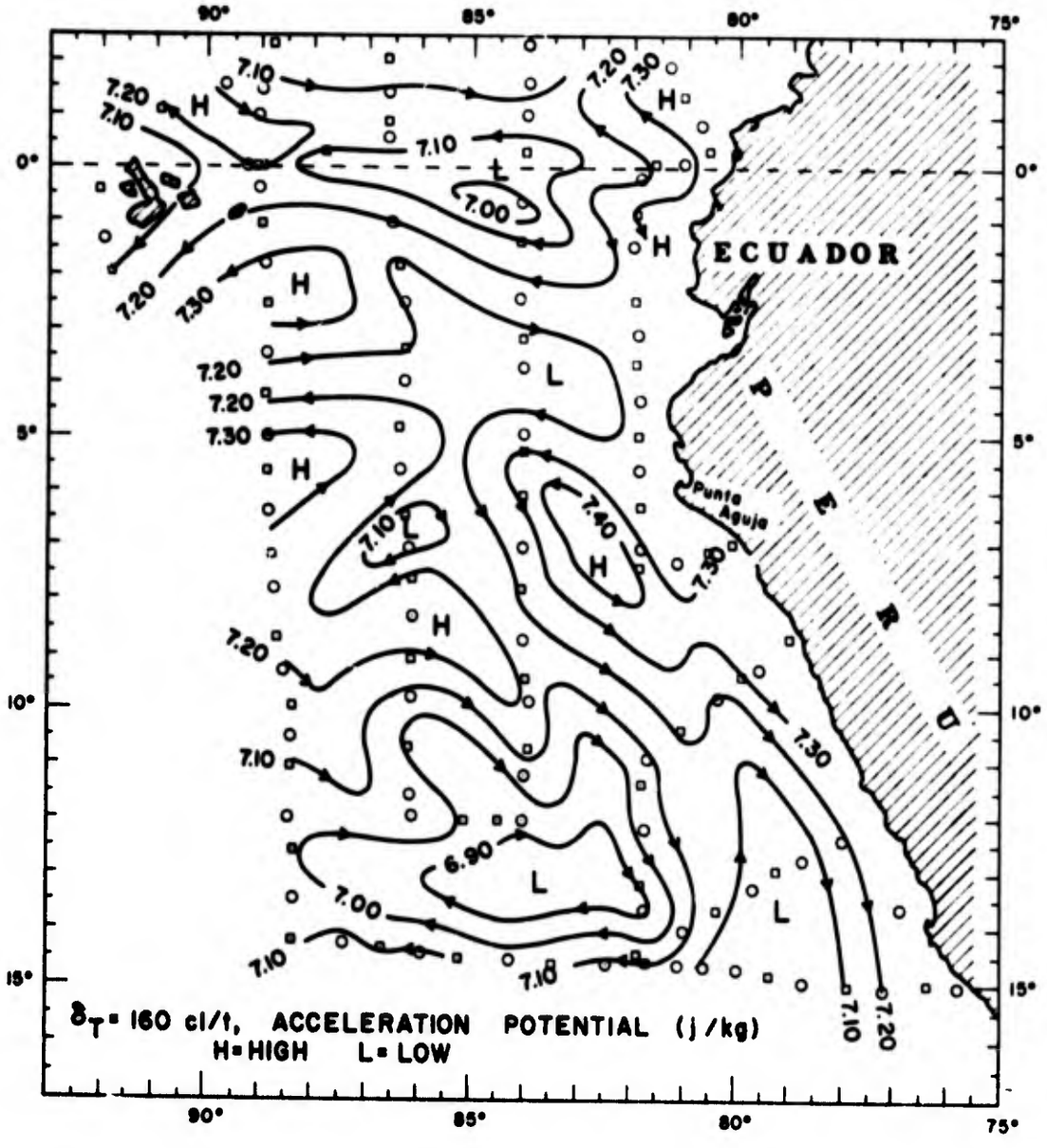

Figure 10(b). Acceleration potential (dynamic decimeters or joules per kilogram) relative to 500 decibars on the surface where $\delta_T = 160$ cl/t.

that at 120 cl/t, although the gradients were larger. Between 2° and 4°S, the south branch of the Equatorial Undercurrent extended to the coast of Peru near 5°S, in a manner similar to that at 120 cl/t. At 5°S, this flow turned seaward and extended to 85°W, where a large portion of it turned south, while the remainder continued out of the region along 5°S. The southward flow at 85°W extended to 10°S, where it returned to the coast. A meander was formed by that portion of flow which extended west at 5°S, southward at 85°W, and returned to the coast near 10°S [figure 10(b)]. Since this important feature of the circulation began near Punta Aguja, it will be referred to by the name, Punta Aguja meander.

Between 9° and 12°S, eastward flow identified at 120 cl/t as the South Equatorial Countercurrent entered the region and extended east, much as it did at the 120 cl/t surface. However, between 6° and 8°S, a strong eastward component of flow was present at 160 cl/t, although not at 120 cl/t. This eastward flow was associated with the corresponding large slopes in the meridional section [figure 2(a)] and appeared to be near the latitudes where Wooster (1961) found the South Equatorial Countercurrent at 95°W. The eastward flow extended to 86°W, where part of it turned north to join the westward flow near 5°S. The remainder continued east to 85°W, where it joined the southward flow of the Punta Aguja meander.

The westward flow along 5°S was in much the same location as that where Wooster (1968) and others have reported the Peru Current turning seaward from the coast. However, it may be noted that the westward flow was not derived from a current flowing north along the Peruvian coast, but rather from the south branch of the Equatorial Undercurrent and the South Equatorial Countercurrent.

Next to the coast of Peru near 10°S, the Peru-Chile Undercurrent was supplied from the west via the Punta Aguja meander. As at the 120 cl/t surface, the Undercurrent extended south to 11°S, where it was joined by flow from the offshoot of the Chile Current, and continued south out of the region near 78°W.

Figure 10(c) shows the distribution of oxygen concentration at the 160 cl/t surface. The range of concentration was higher at 160 cl/t than at 120 cl/t and many of the features of the flow pattern were more clearly shown at 160 cl/t. As the vertical sections and station curves indicate, the 160 cl/t surface lay just below the high oxygen core of the south branch of the Equatorial Undercurrent and at the high oxygen core of the South Equatorial Countercurrent. Between 3° and 4°S, a tongue of high oxygen (> 1.00 ml/l), associated with the South Equatorial Countercurrent, extended east into the region. The tongue, however, went only to 85°W, where it disappeared.

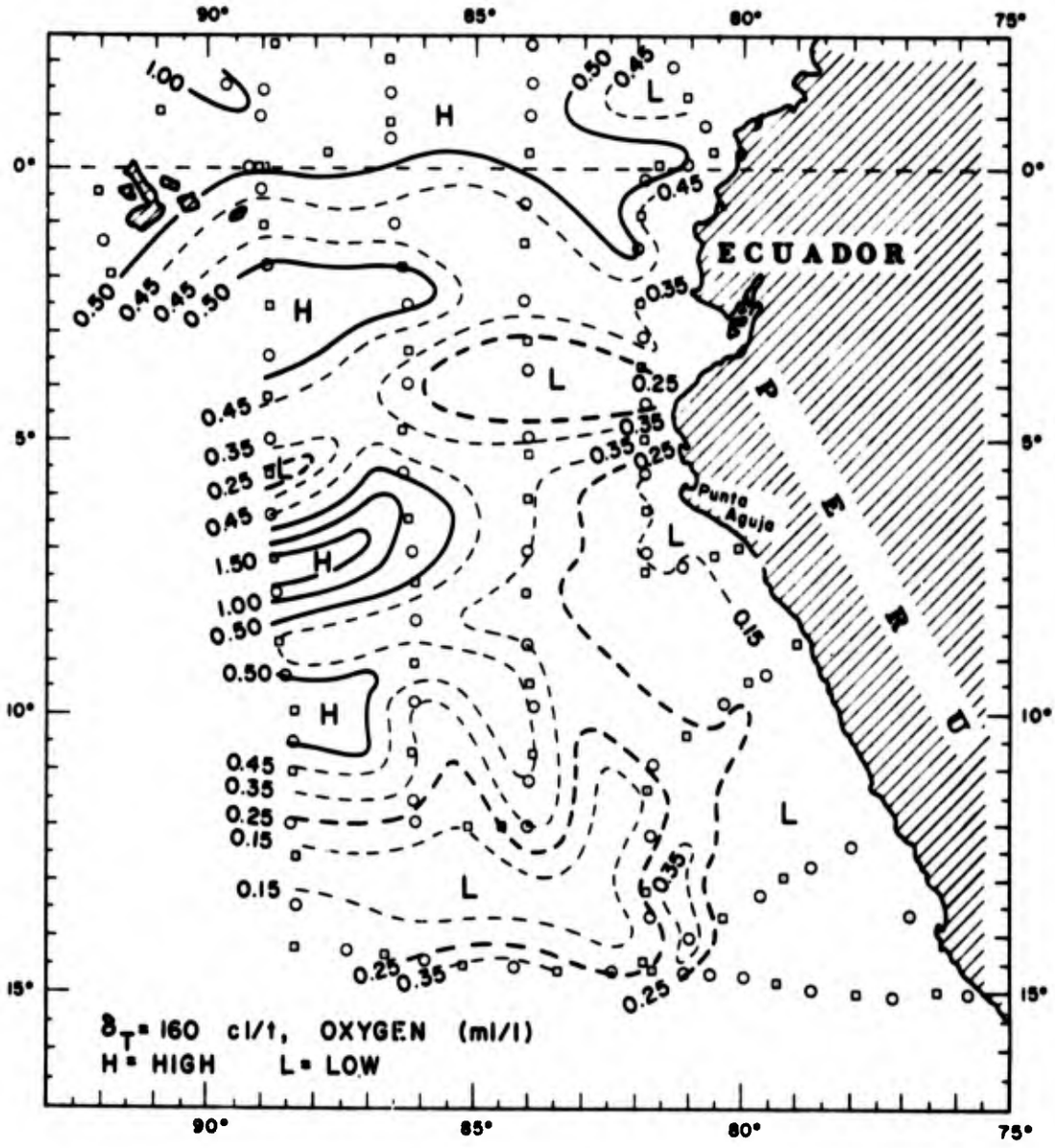

Figure 10(c). Oxygen (milliliters per liter) on the surface where $\delta_T = 160$ cl/t.

The oxygen concentration in the westward flow at 5°S was less than in either of the two neighboring eastward flows.

On the whole, the oxygen concentration at 160 cl/t was lower than at 120 cl/t. Much of the eastern part of the region and the western part south of 11°S was characterized by very low oxygen concentration. The lowest values were found off Punta Aguja and, to a larger extent, in the cyclonic loop between the South Equatorial Countercurrent and the westward extensions of the Chile Current. The low oxygen values between the latter two flows near 160 cl/t formed the oxygen minimum of the entire region, in the vertical as well as in the horizontal.

Figure 10(d) exhibits a salinity distribution at 160 cl/t similar to that at 120 cl/t. A band of high salinity (>34.90 ‰) accompanied the south branch of the Equatorial Undercurrent to the coast of Ecuador near 4°S. Between 6° and 9°S, high salinity (34.92 ‰), associated with the South Equatorial Countercurrent, extended east to 84°W, where it disappeared; this was similar to the situation at 120 cl/t. The westward flow at 5°S was associated with relatively low salinity rather than the high salinity at 120 cl/t.

Next to the coast of Peru south of 6°S, the salinity values (34.94 ‰) were the largest of the region. Since these values were isolated, they apparently resulted from downward mixing. Farther

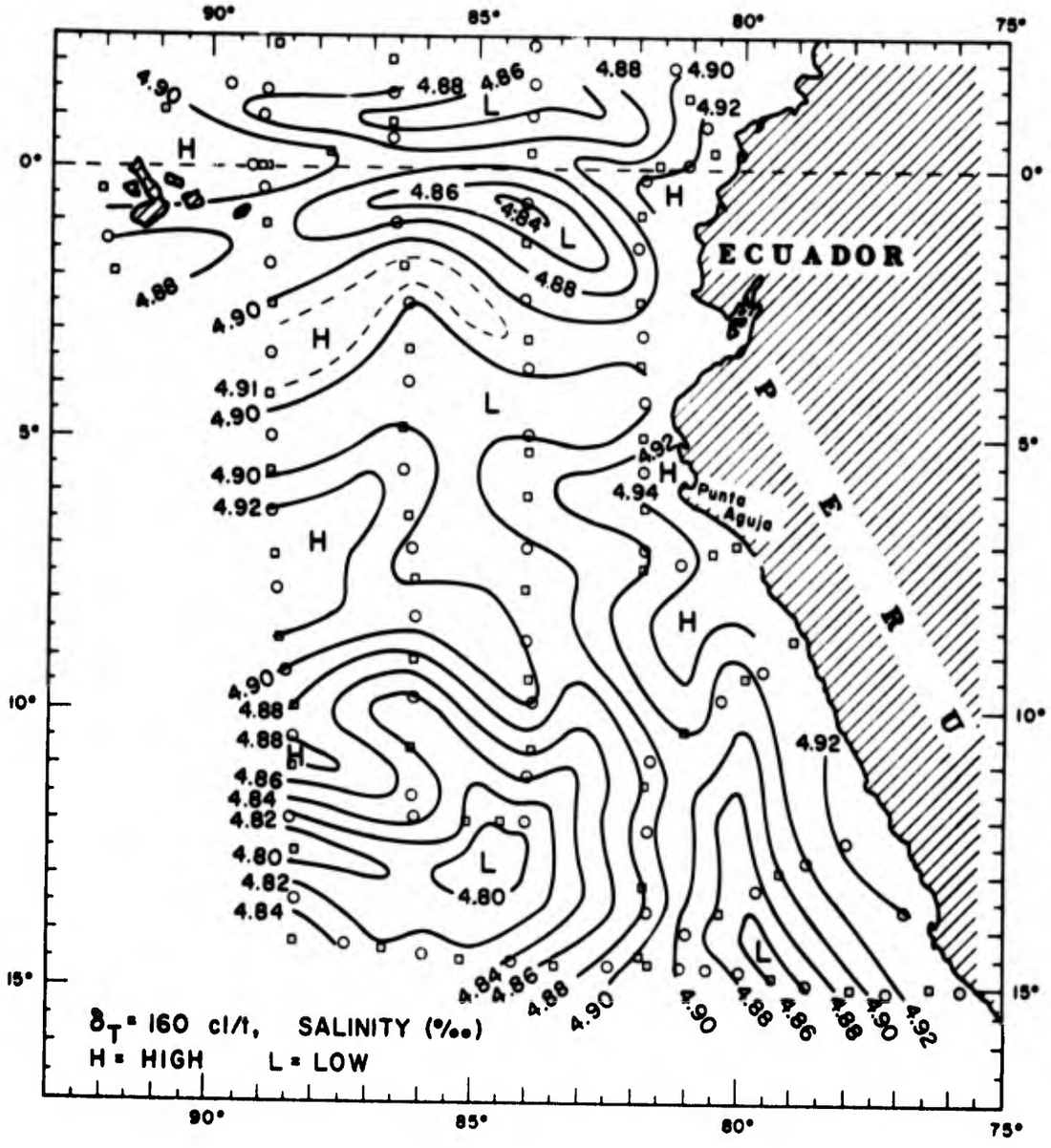

Figure 10(d). Salinity (‰) on the surface where δ_T = 160 clt (add 30.00‰ to salinity values).

south, a ridge of high salinity (34.92‰) extended south along the coast accompanying the Peru-Chile Undercurrent out of the region. Just west of this ridge of high salinity, lower values (< 34.90‰) were carried northward by the offshoot of the Chile Current.

The Equatorial Thermostad Near 180 cl/t

In the chapter on vertical structure, it was noted that the south branch of the Equatorial Undercurrent, at the western edge of the region, was characterized by an equatorial thermostad between 150 and 190 cl/t and an oxygen maximum near 180 cl/t. To follow the equatorial thermostad into the region, the distribution of thickness from 170 to 190 cl/t is shown in figure 11(a). How the oxygen maximum extended into the region can be seen from the distribution of oxygen at 180 cl/t, shown in figure 11(b). The acceleration potential at 180 cl/t was similar to that at 160 cl/t [figure 10(b)].

Between 2° and 3°S, the layer from 170 to 190 cl/t was quite thick along a band (> 120 m) extending east with the south branch of the Equatorial Undercurrent. The thickest part lay between the latter current and the westward flow near the equator. At 85°W, the layer expanded to 160 m, suggesting a piling up of water against the coast. Near 4°S, a tongue of large thickness extended from the coast westward with the flow at that latitude. In association with this large thickness, a tongue of high oxygen (> 2.00 ml/l) extended

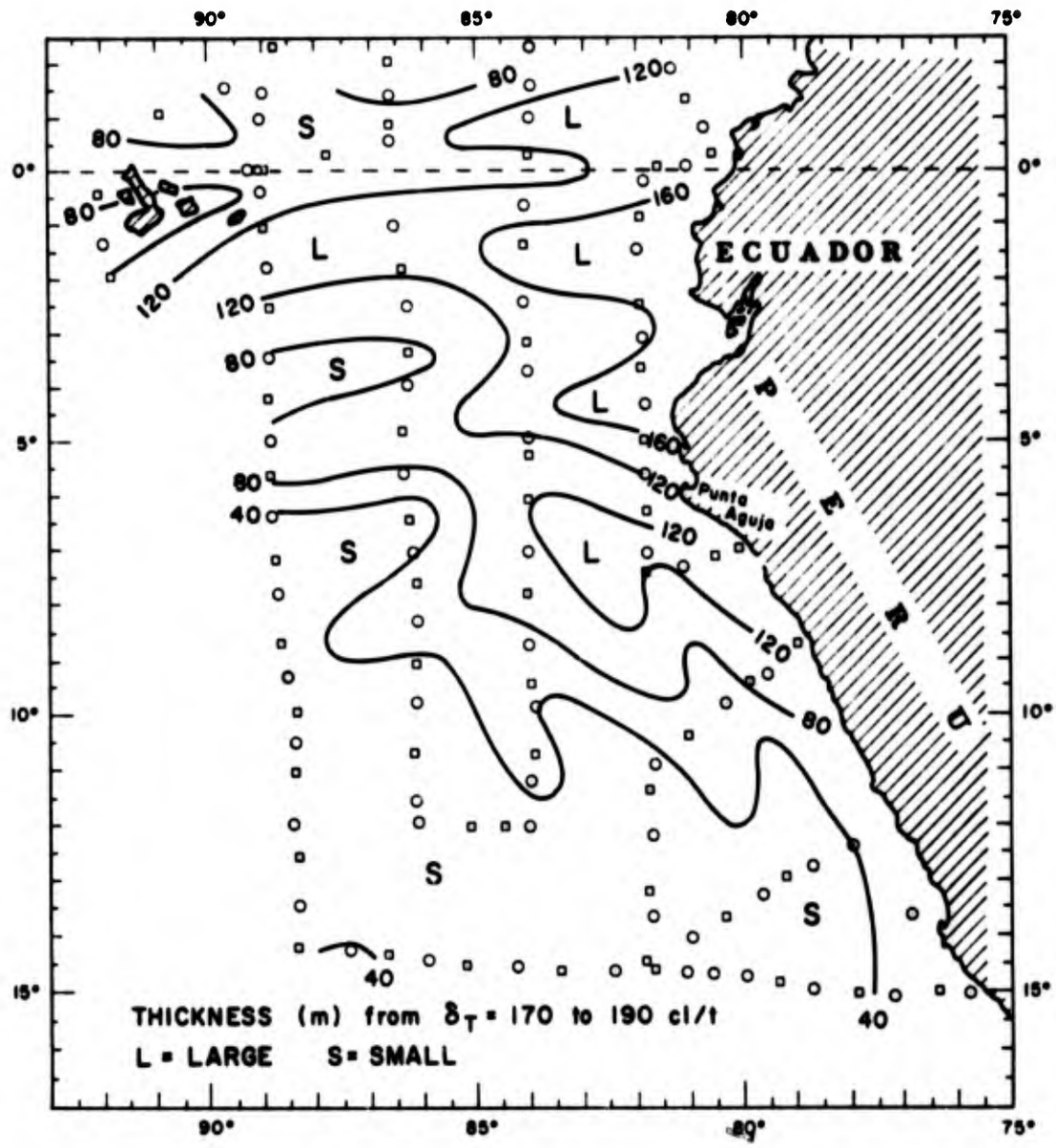

Figure 11(a). Thickness (meters) from δ_T = 170 to 190 cl/t.

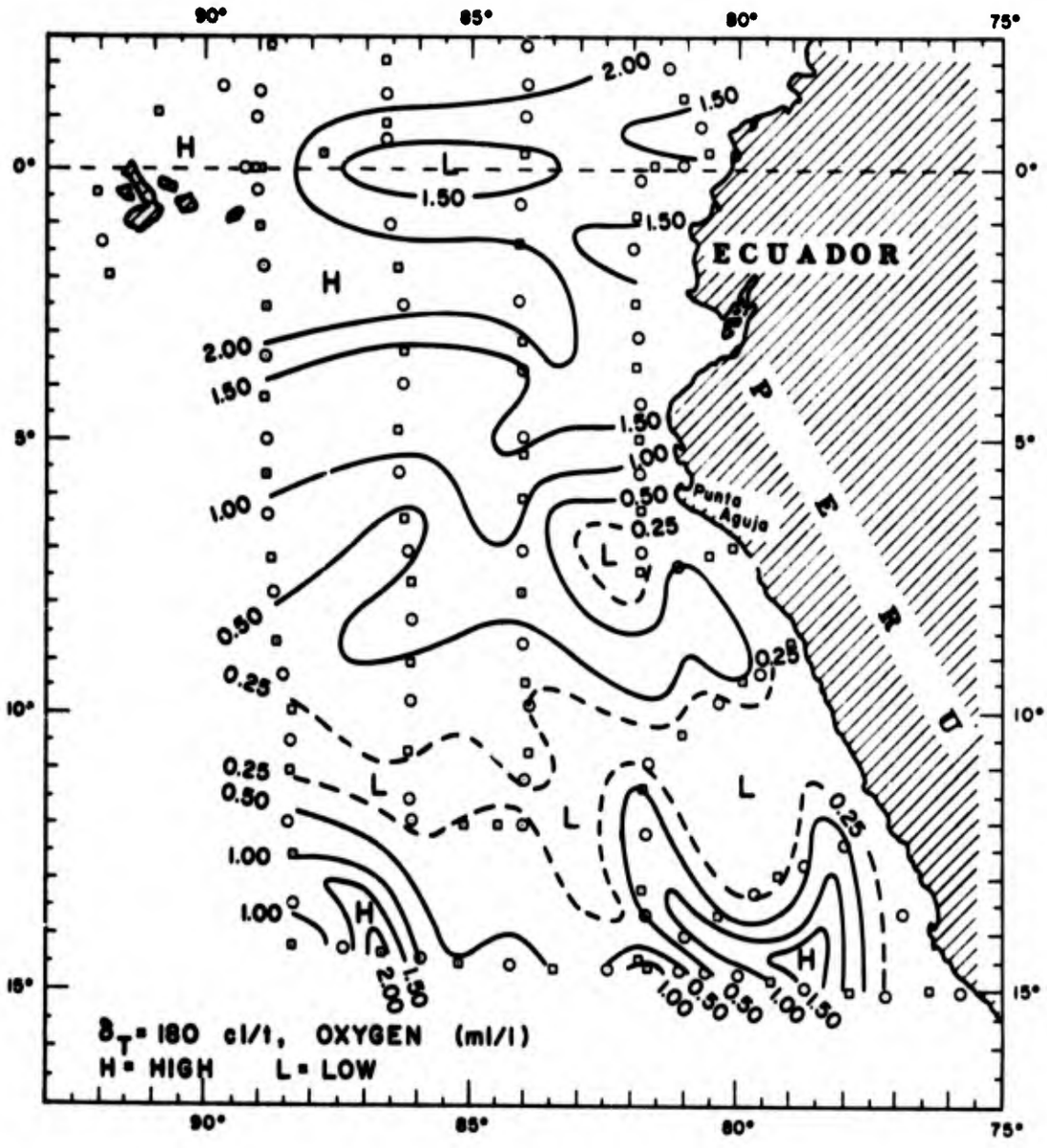

Figure 11(b). Oxygen (milliliters per liter) on the surface where δ_T = 180 cl/t.

into the region between 1° and 3°S along with the south branch of the Equatorial Undercurrent. Near 84°W, the tongue turned south to 5°S and weakened.

Over this segment of flow, the distribution of thickness from 170 to 190 cl/t and the distribution of oxygen at 180 cl/t, in correspondence with the acceleration potential at 160 cl/t, indicates that the south branch of the Equatorial Undercurrent was a rather well defined current during the ALAMINOS cruise. However, the form of the current in the region east of the Galapagos Islands is apparently not constant. Wooster and Cromwell (1958) indicate two bands of high oxygen east of the Galapagos Islands, one at 1°S, and the other at 2°N. On the other hand, Bennett (1963) found high oxygen on both sides of the Galapagos Islands, but east of the islands at 84°W he found only one high oxygen core on the equator.

At 6°S near Punta Aguja, the layer was quite thick (> 120 m) in a small area at the center of the Punta Aguja meander [figure 10(b)]. Around the meander, the layer was still rather thick (80 to 120 m) with values almost the same as those found near 3°S along the south branch of the Equatorial Undercurrent [figure 11(a)]. The high oxygen tongue, which had extended into the region with the south branch of the Equatorial Undercurrent to 5°S, followed the geostrophic flow around the meander, weakening downstream.

Along the coast of Peru south of 9°S, the values of thickness between 80 and 120 extended only as far south as 10°S. Similarly, the high oxygen which came in from the west via the Punta Aguja meander extended only as far south as 10°S, where it disappeared.

At the southern edge of the region, two tongues of high oxygen, one at 79°W and the other at 87°W, entered the region. The tongue at 79°W corresponded to the offshoot of the Chile Current. The tongue near 87°W was apparently associated with the westward extension of the Chile Current. The latter current, as indicated by the high oxygen tongue, extended farther north at 180 cl/t than it did at 160 cl/t.

Because of the tongues of high oxygen just noted, the extent of very low concentrations was smaller at 180 cl/t than at 160 cl/t. The region of low oxygen (< 0.25 ml/l) was restricted to a narrow zone near 11°S, extending from the coast of Peru to the west side of the region. The zone lay primarily in the area between the South Equatorial Countercurrent and the westward extension of the Chile Current, although part of the zone extended to the Peru-Chile Undercurrent near the coast. Thus, although not as extensive, the region of low oxygen was situated rather like that at 160 cl/t. The vertical orientation of the low oxygen zone between the South Equatorial Countercurrent and the westward extension of

the Chile Current may be seen in the meridional section [figure 2(b)], which shows low oxygen values between the high oxygen core of the South Equatorial Countercurrent at about 8°S and the high oxygen of the westward extension of the Chile Current (above 160 cl/t) at 12°S.

The 200 cl/t Surface

Figure 12(a) shows the 200 cl/t surface to lie between 40 and 140 m in depth. The relief of the 200 cl/t surface was gentler than at 160 cl/t and many of the features at 160 cl/t were displaced northward at 200 cl/t. The two troughs, which pushed into the region from the south at 160 cl/t, extended still farther north at 200 cl/t. They represent the increased northward penetration of the westward extension of the Chile Current and its related currents.

Figure 12(b) displays the acceleration potential on the 200 cl/t surface, where the geostrophic speeds were much higher than at deeper surfaces already discussed. In the northern portion of the region, the flow pattern differed little from that at 160 cl/t. The south branch of the Equatorial Undercurrent extended to the coast of Peru near 5°S, where most of the flow continued around the Punta Aguja meander, while the remainder extended out of the region along 5°S. Between 6° and 8°S, the northern part of the South

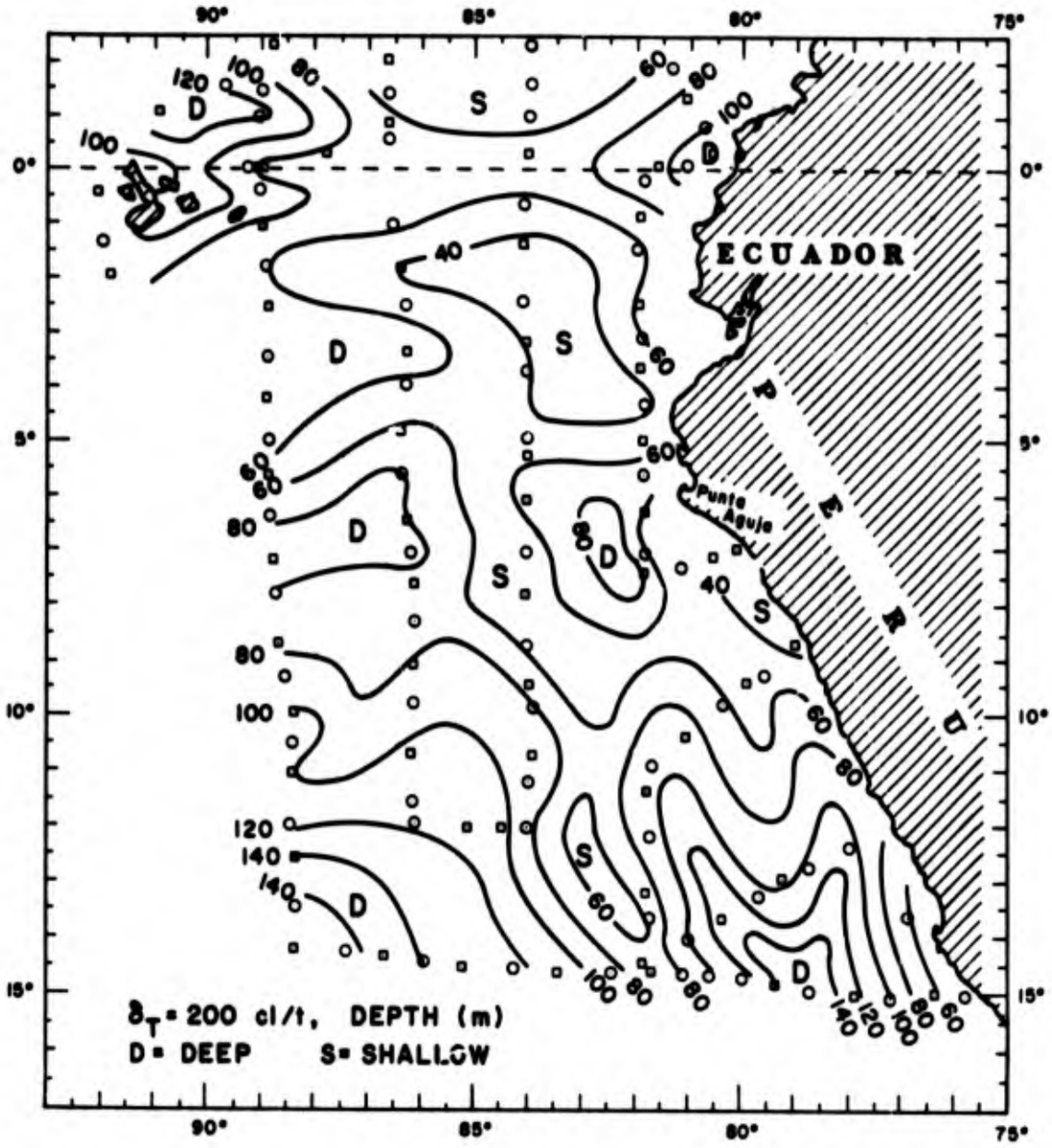

Figure 12(a). Depth (meters) of the surface where $\delta_T = 200$ cl/t.

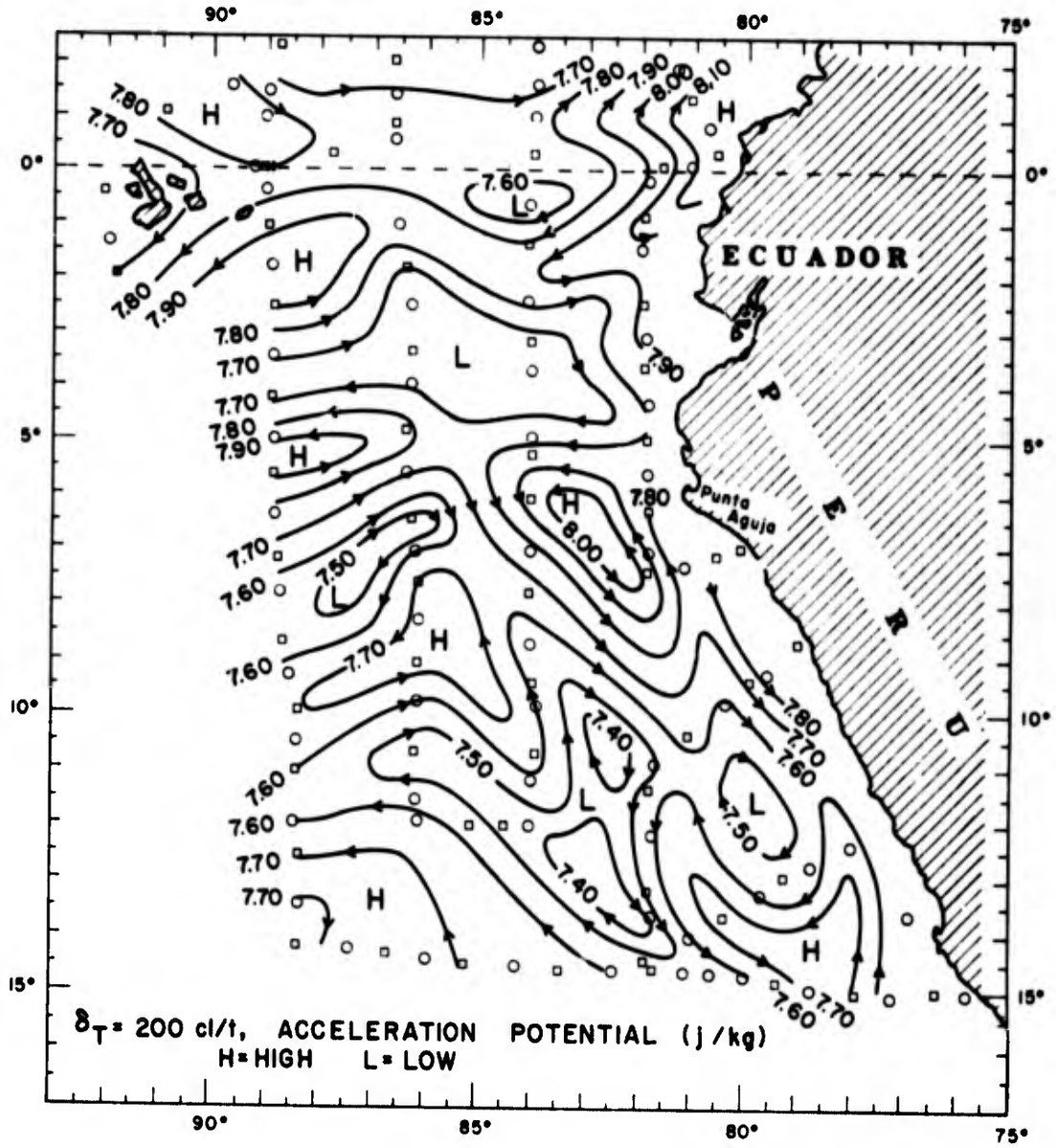

Figure 12(b). Acceleration potential (dynamic decimeters or joules per kilogram) relative to 500 decibars on the surface where $\delta_T = 200$ cl/t.

Equatorial Countercurrent entered the region much as it did on 160 cl/t with, however, a larger proportion of the flow continuing east to join the southward flow of the Punta Aguja meander. Within the meander itself, a fully developed anticyclonic eddy appeared, with definite northward flow along its east side.

Next to the coast of Peru between 8° and 11°S, the Peru-Chile Undercurrent was present. However, the Undercurrent did not extend farther south than 11°S, having been replaced by a northward flow. The northward flow was characterized by relatively high oxygen values [figure 12(c)]. As noted in the discussion of vertical sections, the high oxygen is associated with the Chile Current. Consequently, the northward flow appears to have been an offshoot of the Chile Current, although considerably changed in form from its counterpart at 160 cl/t.

In the western part of the region south of 12°S, the westward extension of the Chile Current passed through the region toward the northwest, whereas at 160 cl/t, it barely extended into the region. As a result, the southern extent of the South Equatorial Countercurrent was decreased. A flow, which might be considered as the southern part of the South Equatorial Countercurrent, entered the region between 10° and 11°S and extended east to 84°W. There, much of the flow went south to form a cyclonic eddy as shown [figure 12(b)],

while the remainder turned north and combined with flow from the northern part of the South Equatorial Countercurrent. The combined flow extended west out of the region between 8° and 10°S, separating the two parts of the South Equatorial Countercurrent.

Wyrtki (1963), in his interpretation of the STEP-I data, described a southward flow nearly 200 miles off the coast of Peru and called it the Peru Countercurrent. Such a flow might be said to have been present during the ALAMINOS cruise. However, the southward flow was found to consist of two segments, with differing water characteristics. Southward flow extended from 6° to 10°S as a part of the Punta Aguja meander and contained water from the south branch of the Equatorial Undercurrent and the South Equatorial Countercurrent. Near 10°S, this flow turned toward the coast to form the Peru-Chile Undercurrent. Another southward flow, roughly aligned with the first, extended from 11° to 15°S along 82°W. It constituted the east side of the cyclonic eddy which lay between the South Equatorial Countercurrent and the westward extension of the Chile Current and contained water from the latter currents. The contrast between the two southward segments of flow is particularly evident in the oxygen distribution at 180 cl/t [figure 11(b)].

Wyrtki (1963) also found that the South Equatorial

Countercurrent did not penetrate to the coast of Peru, because of the southward flow in the Peru Countercurrent. However, the map of acceleration potential shows that flow from the South Equatorial Countercurrent was carried to the coast by way of the Punta Aguja meander, in agreement with the results of Tsuchiya (1968) and Cochrane (1967).

Figure 12(c) shows the distribution of oxygen at 200 cl/t to be much like that at the 180 cl/t surface. North of 5°S, the concentrations were slightly less than those at 180 cl/t, because of a minor oxygen minimum near 200 cl/t in the south branch of the Equatorial Undercurrent, as shown in the station curves for station 150 (figure 4).

Along the southern edge of the region, the two tongues of high oxygen, similar to those at 180 cl/t, were stronger and extended somewhat farther north into the region. The high oxygen tongue (>2.00 ml/l) near 79°W was carried north to 11°S by the offshoot of the Chile Current described above. The tongue of high oxygen (>3.00 ml/l) near 87°W was carried northward by the westward extension of the Chile Current. Apparently, part of this water of high oxygen concentration was returned to the east along 11°S by the southern part of the South Equatorial Countercurrent.

Between the high oxygen in the northern part of the region

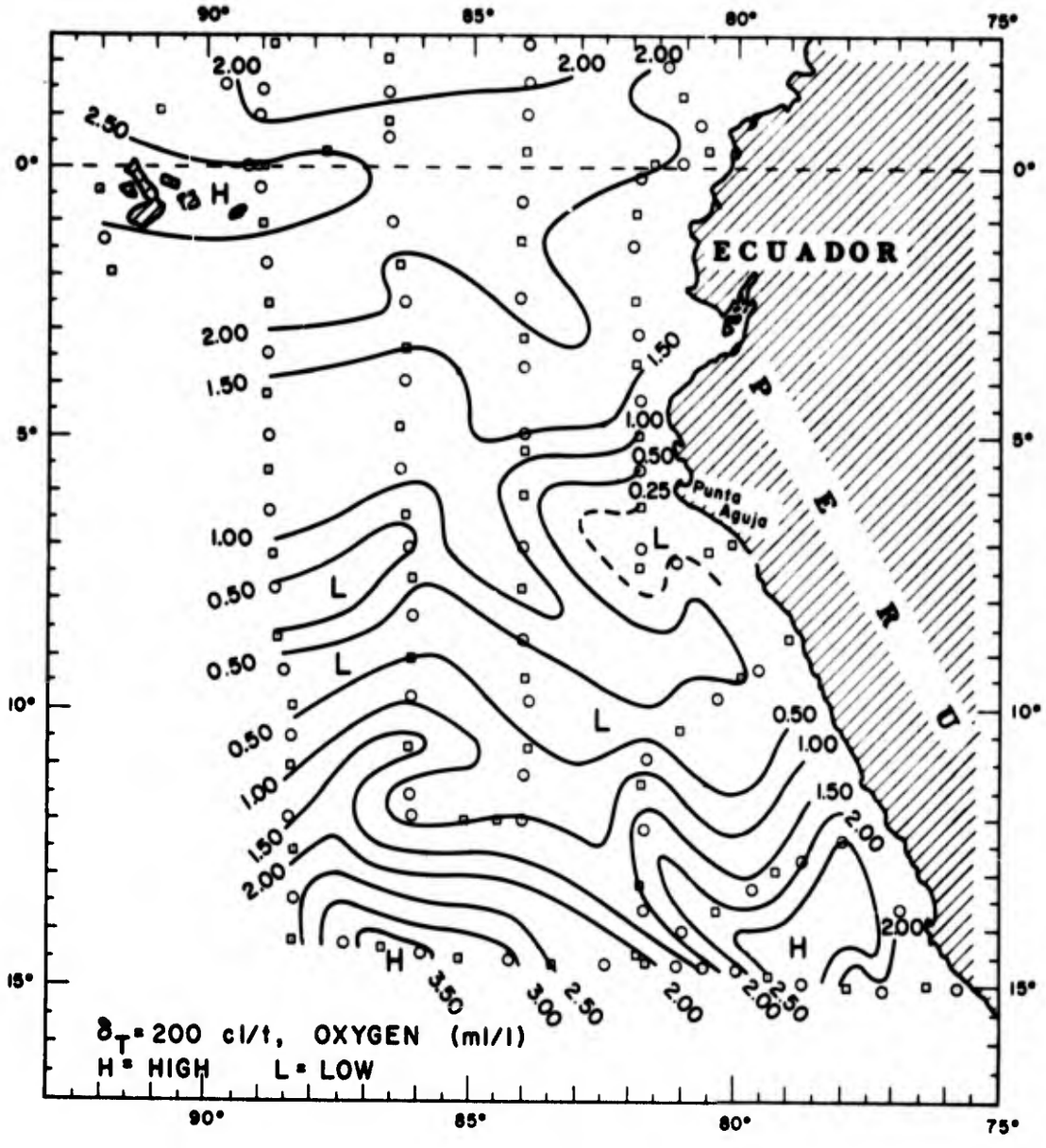

Figure 12(c). Oxygen (milliliters per liter) on the surface where $\delta_T = 200$ cl/t.

and that extending into the region from the south, there was a zone of low oxygen situated much as the corresponding zone at 180 cl/t, but displaced somewhat farther north.

The 280 cl/t Surface

Figure 13(a) shows the 280 cl/t surface to lie between 20 and 50 m in depth. Although the depth range was much smaller than at 200 cl/t, the main features were quite similar. Next to the coast of southern Peru, the trough associated with the offshoot of the Chile Current extended farther north (to 9°S) than on the surfaces already discussed.

Figure 13(b) displays the acceleration potential at the 280 cl/t surface. It is remarkably similar to that at 200 cl/t with one noticeable difference, the increased northward extent (to 10°S) of the offshoot of the Chile Current and the corresponding disappearance of the Peru-Chile Undercurrent south of 10°S.

Because the 280 cl/t surface lay fairly close to the sea surface and the isanosteric surfaces above it largely conformed to its shape [figures 2(a) and 3(a)], the circulation pattern at 280 cl/t may be considered similar to the geostrophic pattern near the sea surface. In Wyrtki's (1965) chart for the average surface currents (based on observations of surface drift by ships) for March, the

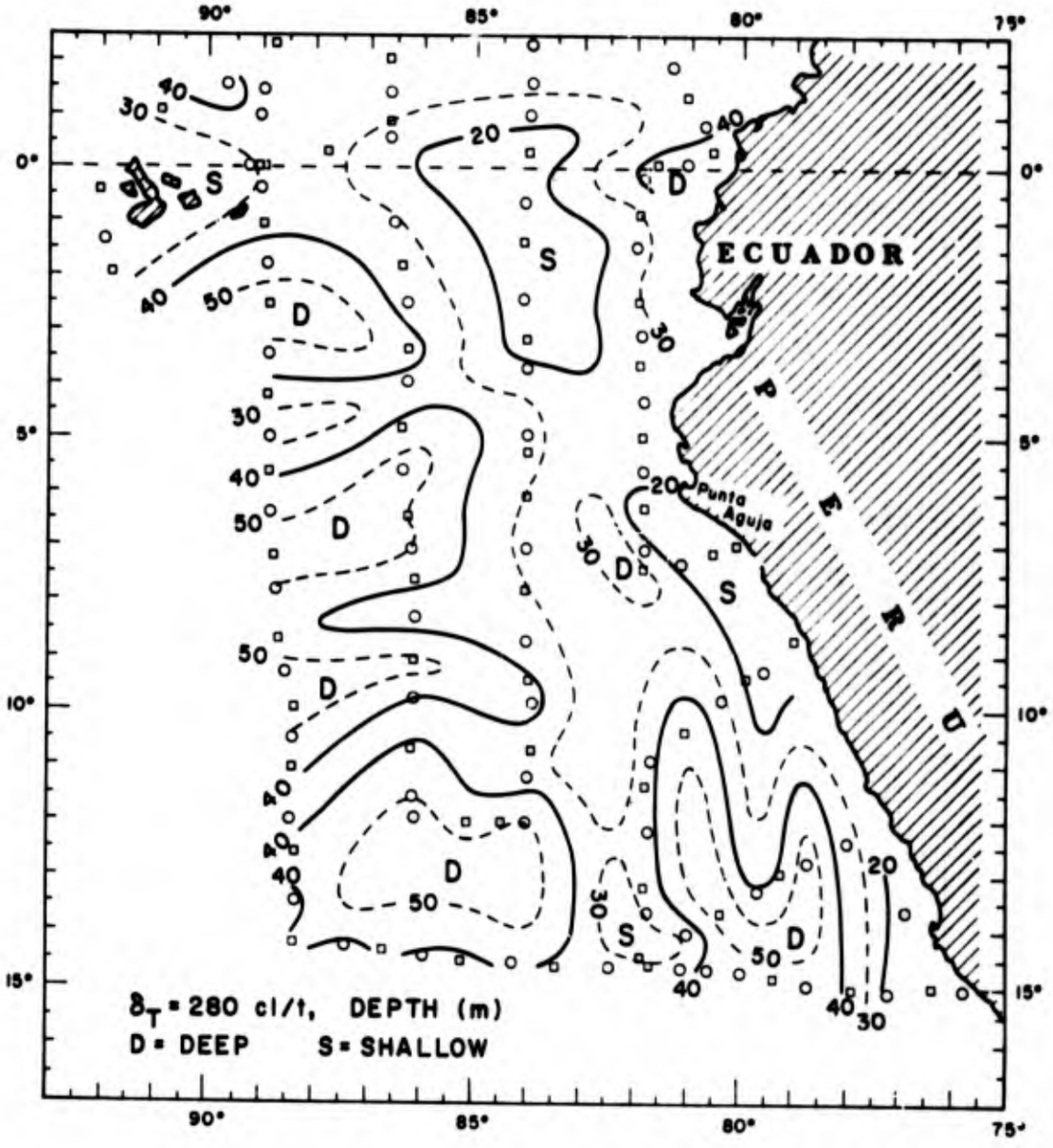

Figure 13(a). Depth (meters) of the surface where $\delta_T = 280$ cl/t.

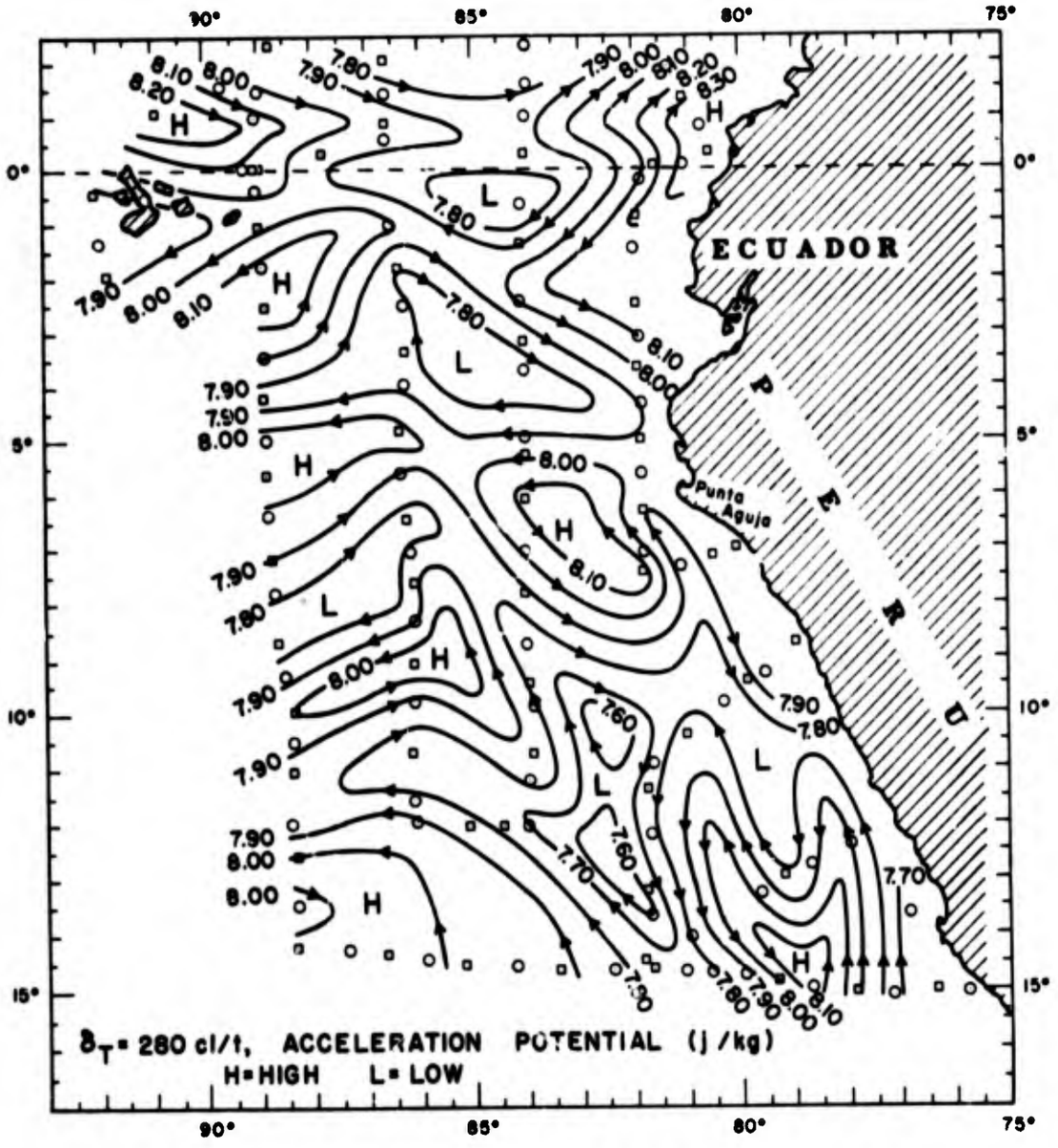

Figure 13(b). Acceleration potential (dynamic decimeters or joules per kilogram) relative to 500 decibars on the surface where δ_T = 280 cl/t.

southward flow at roughly 200 miles off Peru between 5° and 15°S may be seen. This flow, which Wyrtki called the Peru Countercurrent, has already been discussed for 200 cl/t. At 280 cl/t next to the coast in the southern part of the region, a northward flow extended to 11°S, turned west to 80°W, and continued a little farther north to 10°S. At 9°S a second northward flow, roughly aligned with the first, extended along the east side of the Punta Aguja meander to 5°S, where it turned west. These two segments of flow, taken together, agree to a considerable extent with the Peru Current as shown in Wyrtki's (1965) surface current chart for March, although the two segments at 280 cl/t were found to have different water characteristics.

On the other hand, such average sea-surface current charts as those of Wyrtki (1965) indicate that for March the south branch of the Equatorial Undercurrent and the South Equatorial Countercurrent are masked near the surface by the drift induced by the southeast trade winds.

Figure 13(c) shows the oxygen concentration at 280 cl/t to have considerably higher values than at 200 cl/t, because much of the 280 cl/t surface was within the high oxygen regime extending down from the sea surface. Between the equator and 3°S, high oxygen (>3.00 ml/l) was found in the zone occupied by the south

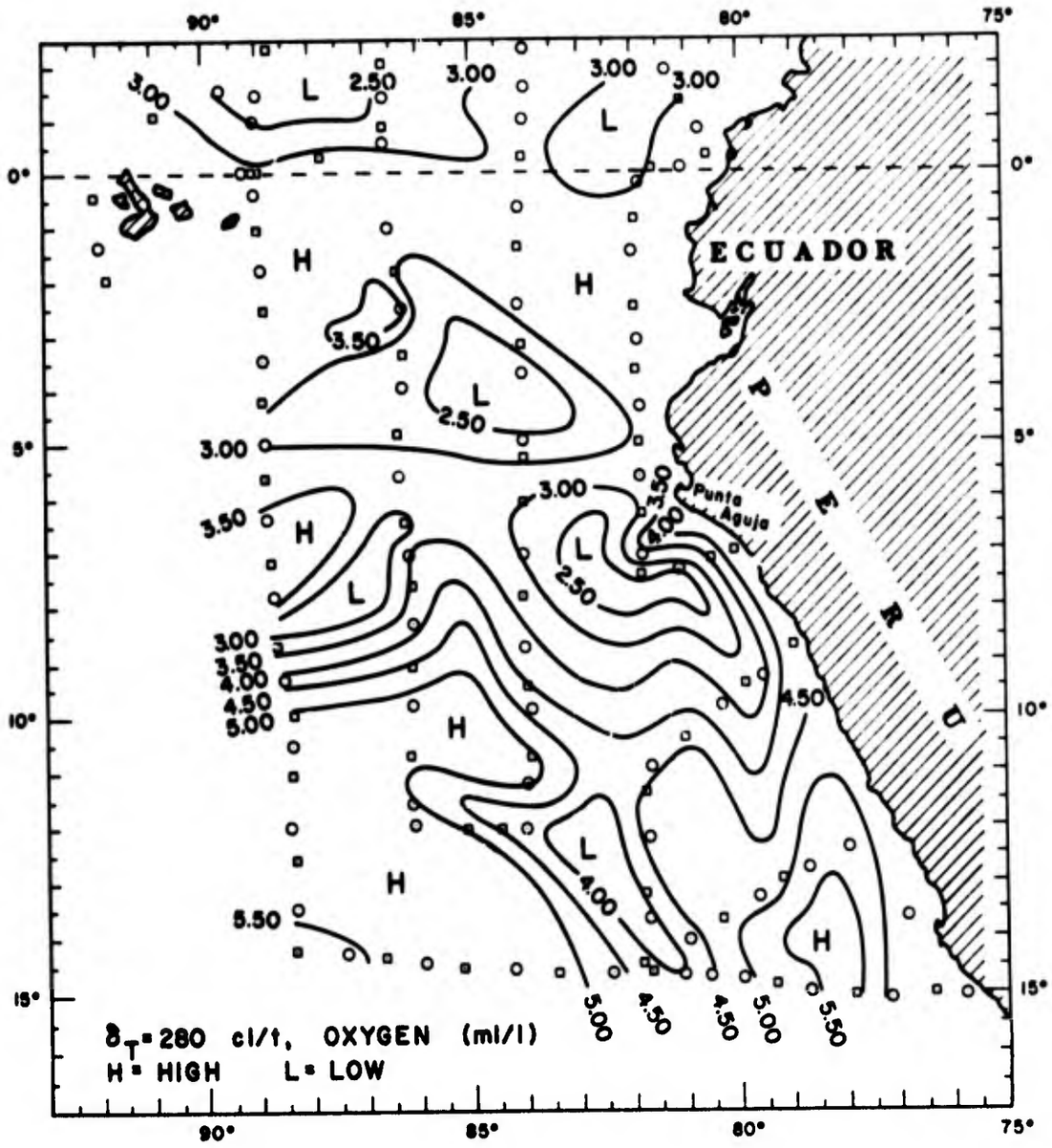

Figure 13(c). Oxygen (milliliters per liter) on the surface where δ_T = 280 cl/t.

branch of the Equatorial Undercurrent. Next to the coast, high oxygen values extended south to 6°S, where they turned west to form a band following the westward flow near that latitude.

From the southern edge of the region, high oxygen (>5.00 ml/l) associated with the offshoot of the Chile Current extended north along the coast to 10°S. This high oxygen replaced the rather low oxygen next to the coast of Peru between 5° and 10°S found at 200 cl/t. West of 84°W, similar high oxygen (>5.00 ml/l) extended as far north as 9°S, indicating the increased northward penetration of the westward extension of the Chile Current. Separating these two areas of high oxygen was a region of low oxygen (<4.00 ml/l) between 81° and 83°W, where a cyclonic eddy is shown by the acceleration potential [figure 13(b)].

CHAPTER IV

VOLUME TRANSPORTS

In the preceding chapter, the circulation patterns on isanosteric surfaces are illustrated. To show further interrelationships among the important currents and to indicate their continuity of flow, transports relative to 500 db are calculated for each of the sections shown in figure 14. For each section, table I gives the transports between various isanosteric surfaces and the total for the section.

The south branch of the Equatorial Undercurrent is represented by the transports for section I between stations 148 and 152. The transports show a maximum (4.4 sv) for the layers between 160 and 200 cl/t, which approximate the equatorial thermostad.

The south branch of the Equatorial Undercurrent continued east to about 86°W, where it turned southward. Section II between stations 49 and 303 is used to represent the flow in that area. The transport there was less than at the previous section, although the transport maximum was in the same layers. The acceleration potential for all the isanosteric surfaces indicates some loss from the Undercurrent to the westward flow near the equator.

The South Equatorial Countercurrent is represented in table I

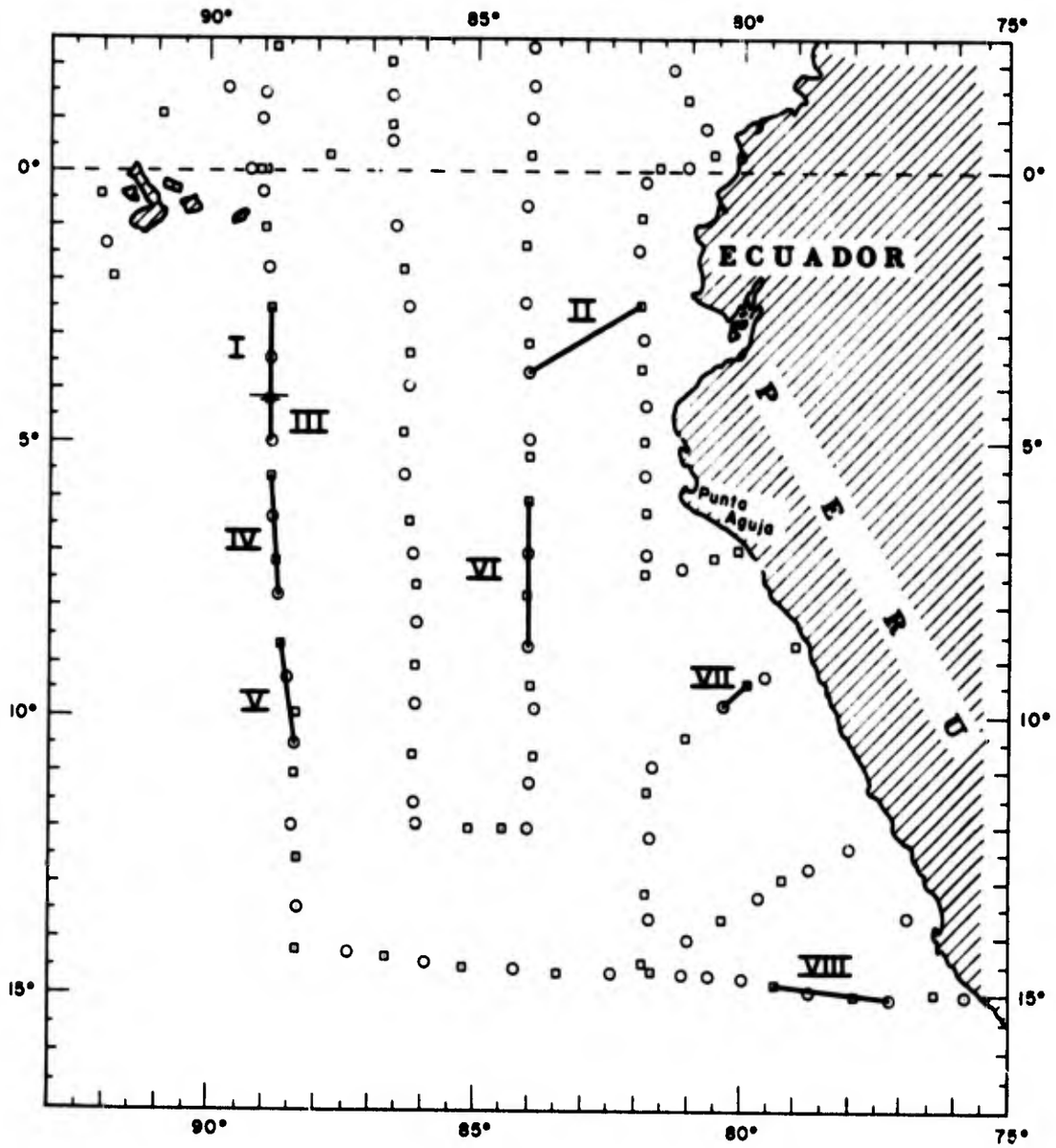

Figure 14. Location of volume transport calculations.

TABLE I

Volume Transports* (sv)

at the Locations Given in Figure 14

Location (Station Number) $\Delta\delta_T$ (cl/t)	I (148-152)	II (49-303)	III (146-148)	IV (144-138)	V (132-136)	VI (291-297)	VII (77-78)	VIII (93-99)
240-280	0.2 (sv)	0.3	-0.2	0.1	-0.1	0.2	0.1	-0.2
200-240	0.7	0.5	-0.6	0.3	-0.1	0.4	0.2	-0.3
180-200	2.0	1.9	-0.8	0.8	0.0	1.2	0.4	0.0
160-180	2.4	2.1	-2.0	1.2	0.2	2.3	1.2	0.2
140-160	0.9	0.6	-1.4	0.6	0.5	0.7	0.4	0.5
120-140	0.4	0.3	-0.7	0.1	0.1	0.1	0.2	0.3
Net Total	6.6 (sv)	5.7	-5.7	3.1	0.6	4.9	2.5	0.5

*Positive transports indicate eastward or southward direction, while negative transports indicate northward or westward direction.

by the sections IV and V between stations 138 and 144, and between stations 132 and 136, respectively. Of a total eastward transport of 3.9 sv through both sections, the largest part was found in the northern section (IV). There, a transport maximum was found between 160 and 180 cl/t in the upper thermostad, which was indicated in the station curves for station 140 (figure 5). The eastward transport at section IV in the southern part of the current was 0.8 sv and was confined to the layers below 200 cl/t. Above those layers, there was a small westward transport.

The westward transport out of the region near 5°S, calculated for section III between stations 146 and 148, had a maximum in the layer between 140 and 180 cl/t. This maximum could be accounted for by that of the south branch of the Equatorial Undercurrent. However, the acceleration potentials indicate contributions to the westward flow from not only the south branch of the Equatorial Undercurrent, but also the South Equatorial Countercurrent.

The southward flow in the Punta Aguja meander was composed of water from both the south branch of the Equatorial Undercurrent and the South Equatorial Countercurrent. The transport of the southward flow in the meander at section VI between stations 291 and 297 reached a maximum (3.5 sv) in the layer from 160 to 180 cl/t. This maximum was in the lower part of the layer for which

the south branch of the Equatorial Undercurrent reached a maximum and in the same layer as that for which the South Equatorial Countercurrent showed a maximum. Thus, the maximum could be accounted for by the transports of the latter two currents.

The maps of acceleration potential show that the southward flow in the meander returned to the coast near 10°S to form the Peru-Chile Undercurrent. The southward transport of this flow at section VII between stations 77 and 78 was found to be about half of that in the southward flow around the meander, although the maximum was found in the same layer (160-180 cl/t). Since the depth between station 77 and the coast was less than 500 m, the transport was not calculated and, as a result, a significant amount of the southward transport may not appear in table I.

Farther south at 15°S in section VII between stations 93 and 99, the southward transport of the Peru-Chile Undercurrent was confined to the layers below 200 cl/t, with no appreciable maximum anywhere in the column. Above 200 cl/t, there was a small northward transport associated with the offshoot of the Chile Current.

CHAPTER V

SUMMARY

During the ALAMINOS cruise of the EASTROPAC studies, the south branch of the Equatorial Undercurrent entered the region between 3° and 4°S. Above 120 cl/t, the current extended northeast to 86°W near the equator at 2°S. There, some of the flow joined a westward current along the equator; however, most turned southeast and continued to 3°S near the coast, where it was joined by a small southward flow from the vicinity of the equator. From 3°S, the combined flow extended farther south to the coast of Peru near 5°S. Throughout this segment of flow, the geostrophic speed increased upward from 120 to 280 cl/t. The flow was characterized by an equatorial thermostad between 150 and 190 cl/t, which increased in thickness toward the coast. In the upper thermostad near 180 cl/t, there was a high oxygen core, which weakened only slightly toward the west. Within the thermostad, the volume transport reached a maximum value.

Near 5°S adjacent to the coast of Peru, the above mentioned southward flow turned seaward and extended to 84°W, where a large part of this westward flow turned south while the remaining flow continued west and passed out of the region near 5°S. The southward flow at 84°W extended to the vicinity of 10°S, where it returned to

the coast. The departure from the coast of the southward flow and its return has been referred to as the Punta Aguja meander. On the west side of the meander, flow from the South Equatorial Countercurrent joined the southward flow.

The South Equatorial Countercurrent entered the region at 120 cl/t as a broad eastward flow between 6° and 13°S. At successive surfaces above 120 cl/t, the southern edge of this current lay progressively farther north as the westward extension of the Chile Current penetrated farther into the region. Above 160 cl/t, the largest portion of eastward flow lay between 6° and 8°S and extended east to 86°W. There, some of the flow turned north to join the westward current along 5°S, while the remaining part continued east to 85°W and joined the southward flow in the Punta Aguja meander. Within this northern part of the South Equatorial Countercurrent, the geostrophic speed increased upward from 120 to 200 cl/t. The flow was characterized by a thermostad between 120 and 180 cl/t and a core of high oxygen near 160 cl/t. Both of these features decreased markedly toward the east. Within the upper thermostad between 160 and 180 cl/t, the volume transport reached a maximum.

The westward current extending out of the region near 5°S was fed by both the south branch of the Equatorial Undercurrent and the South Equatorial Countercurrent as already noted. Near

89°W, this flow was characterized by a thermostad between 140 and 200 cl/t and two minor oxygen maxima at 150 and 190 cl/t. In the upper thermostad between 160 and 180 cl/t, the volume transport reached a maximum.

The southward flow of the Punta Aguja meander, as previously noted, extended from 5° to 10°S and was fed by the two eastward flows. Over the segment of flow, the geostrophic speed increased upward from 120 to 200 cl/t. Within the water column, the equatorial thermostad lay between 160 and 190 cl/t, with a high oxygen core situated near 180 cl/t. Downstream, the thermostad thickness remained constant, while the high oxygen decreased appreciably. Within the thermostad, the volume transport reached a maximum.

The Peru-Chile Undercurrent was formed next to the coast between 7° and 10°S by flow via the Punta Aguja meander. Below 180 cl/t, the Undercurrent extended south along the coast and out of the region at 15°S. Near 11°S, a contribution from the offshoot of the Chile Current joined the Undercurrent. Above 180 cl/t, the Undercurrent did not extend farther south than 11°S, having been replaced by the offshoot of the Chile Current, which differed from that at 160 cl/t and pushed north along the coast. At the beginnings of the Peru-Chile Undercurrent near 10°S, the geostrophic speed increased upward from 120 to 180 cl/t. The flow was characterized,

at that location, by the equatorial thermostad between 160 and 190 cl/t. This thermostad was associated with a weak core of high oxygen (0.50 ml/l), which extended only as far south as 11°S, where it disappeared. In the equatorial thermostad, the volume transport reached a maximum. At 15°S, the southward flow was confined to the layer below 180 cl/t with a maximum geostrophic speed at 160 cl/t. At this location, the Peru-Chile Undercurrent was characterized by relatively low oxygen and high salinity.

REFERENCES

Bennett, E. B.
1963. An oceanographic atlas of the eastern tropical Pacific Ocean, based on data from the EASTROPIC Expedition, Oct.-Dec. 1955. Inter-American Tropical Tuna Commission Bulletin 8(2): 165 pp.

Carptenter, J. H.
1965. The Chesapeake Bay Institute technique for Winkler dissolved oxygen method. Limnol. Oceanogr., 10: 141-143.

Cochrane, J. D. and S. Zuta
1969. Equatorial currents east of the Galapagos Islands during February-March, 1967. Unpubl. Manuscript.

Cromwell, T., R. B. Montgomery, and E. D. Stroup
1954. Equatorial Undercurrent in the Pacific Ocean revealed by new methods. Science, 119: 648-649.

Gunther, E. R.
1936. A report on oceanographic investigation in the Peru Coastal Current. Discovery Reports. Cambridge University Press, 13: 107-276.

Knauss, T. A.
1966. Further measurements and observations on the Cromwell Current. J. Mar. Res., 24: 205-239.

Montgomery, R. B.
1938. Circulation in the upper layers of the southern north Atlantic deduced with the use of isentropic analysis. Papers in Phys. Oceanogr. and Mar. Meteorol., W.H.O.I. and M.I.T., 6(2): 55 pp.
1962. Equatorial Undercurrent in review. J. Oceanogr. Soc. Japan, 20th Ann. Vol.: 487-498.

Montgomery, R. B., and W. S. Wooster
1954. Thermosteric anomaly and the analysis of oceanographic data. Deep-Sea Res., 2: 63-70.

Montgomery, R. B., and E. D. Stroup
1962. Equatorial waters and currents at 150°W in July-Aug. 1952. Johns Hopkins Oceanogr. Studies, No. 1, 85 pp.

Reid, J. L.
1959. Evidence of a South Equatorial Countercurrent in the Pacific Ocean. Nature, 184: 209-210.
1965. Intermediate waters of the Pacific Ocean. Johns Hopkins Oceanogr. Studies, No. 2, 85 pp.

Seitz, R. C.
1967. Thermostad, the antonym of thermocline. J. Mar. Res., 25: 203.

Tsuchiya, M.
1968. Upper waters and circulation of the intertropical Pacific Ocean. Johns Hopkins Oceanogr. Studies, No. 4, 50 pp.

Wooster, W. S.
1961. Further evidence of a Pacific South Equatorial Countercurrent. Deep-Sea Res., 8: 294-297.
1968. Eastern boundary currents in the South Pacific. Presented at Score symposium on scientific exploration of the South Pacific, June 18-20. 11 pp.

Wooster, W. S., and T. Cromwell
1958. An oceanographic description of the eastern tropical Pacific. Bull. of Scripps Inst. of Oceanogr., 7(3): 169-281 pp.

Wooster, W. S., and M. Gilmartin
1961. The Peru-Chile Undercurrent. J. Mar. Res., 19: 97-122.

Wooster, W. S., and J. L. Reid
1963. Eastern boundary currents. In The Sea, Vol. 2, M.N. Hill (ed.). Interscience Publ., N.Y., 253-280.

Wyrtki, K.

1963. The horizontal and vertical fields of motion in the Peru Current. Bull. Scripps Inst. of Oceanogr., 8(4): 313-346.

1965. Surface currents of the eastern tropical Pacific Ocean. Inter-American Tropical Tuna Commission Bulletin, 9(5): 271-303.

1966. Oceanography of the eastern equatorial Pacific. Oceanogr. Mar. Bio. Ann. Rev., 4: 33-68.

Yoshida, K.

1967. Circulation in the eastern tropical oceans with special refernce to upwelling and undercurrents. Japanese Jour. of Geophysics, 4(2): 75 pp.

UNCLASSIFIED
Security Classification

DOCUMENT CONTROL DATA - R & D

(Security classification of title, body of abstract and indexing annotation must be entered when the overall report is classified)

1. ORIGINATING ACTIVITY *(Corporate author)*
Department of Oceanography
Texas A&M University, College Station, Texas
Through the Texas A & M Research Foundation

2a. REPORT SECURITY CLASSIFICATION
UNCLASSIFIED

2b. GROUP
UNCLASSIFIED

3. REPORT TITLE
THE EQUATORIAL UNDERCURRENT, THE SOUTH EQUATORIAL COUNTER-CURRENT, AND THEIR EXTENSIONS IN THE SOUTH PACIFIC OCEAN EAST OF THE GALAPAGOS ISLANDS DURING FEBRUARY-MARCH, 1967

4. DESCRIPTIVE NOTES *(Type of report and inclusive dates)*
Technical Report

5. AUTHOR(S) *(First name, middle initial, last name)*
Warren B. White

6. REPORT DATE	7a. TOTAL NO. OF PAGES	7b. NO. OF REFS
May, 1969	74	23

8a. CONTRACT OR GRANT NO.	9a. ORIGINATOR'S REPORT NUMBER(S)
2119(04)	69-4T
b. PROJECT NO. 286-3	
c.	9b. OTHER REPORT NO(S) *(Any other numbers that may be assigned this report)*
d.	

10. DISTRIBUTION STATEMENT
This document has been approved for public release and sale; its distribution is unlimited.

11. SUPPLEMENTARY NOTES	12. SPONSORING MILITARY ACTIVITY
	Office of Naval Research Washington, D. C.

13. ABSTRACT

During February and March 1967, oceanographic observations taken by the R/V ALAMINOS east of the Galapagos Islands and north of 15°S covered the region more completely than previous cruises. The Equatorial Undercurrent was present as two branches, one north and the other south of the equator. This study deals with the circulation and water in the region south of the equator. They are studied by means of vertical sections, station curves, and distributions of properties on isanosteric surfaces from 120 to 280 cl/t. At selected locations volume transports are calculated.

The south branch of the Equatorial Undercurrent extended east between 2° and 4°S from the Galapagos Islands to the coast of Peru. There near 5°S, the flow turned west and reached to about 84°W, where it divided. While some of the flow continued west out of the region near 5°S, the greater part turned south, extended to about 10°S, and returned to the coast. There the flow turned south to form the Peru-Chile Undercurrent, which extended out of the region at 15°S.

Between 6° and 13°S, the South Equatorial Countercurrent entered the region. At 120 cl/t, the flow lay primarily between 11° and 13°S, but from 160 cl/t upward the main eastward flow was between 6° and 8°S. The current extended east to 86°W, where some of the flow joined the westward flow near 5°S. The remainder continued east to 84°W, where it joined the southward flow leading into the Peru-Chile Undercurrent.